A PEDOLOGICAL STUDY OF SOIL GENESIS ON SKIDAWAY ISLAND

by

CHRISTOPHER P. VANAGS

(Under the Direction of William P. Miller and David B. Wenner)

ABSTRACT

Skidaway, a Pleistocene-aged barrier island, was chosen to study the transition between a Talquin fine sand (Arenic Alaquod) and an Ocilla loamy sand (Umbric Paleaquult) in a 15- by 40-m area. The objective was to characterize a young, heterogeneous landscape, which contained a soil association commonly found in older deposits inland. A detailed topographic map was generated, and the subsurface mapped with ground penetrating radar (GPR). GPR profiles were compiled to produce vertical slices, which were used to map the soil boundary. Exchangeable and soluble cations were measured for six profiles. Electrical conductivity, pH, gravimetric moisture, and particle size distribution were determined at 5 m increments over the grid. A 10% clay increase dramatically attenuated the GPR signal, producing slice images that resolve the boundary within 20 cm. An extensive microdepression corresponded with a change in parent material across the grid and at depth. Geochemical analysis showed order-or-magnitude shifts in pH and cation exchange capacity reflected by changes in vegetation at the boundary.

INDEX WORDS: Ground-penetrating radar, barrier islands, coastal soils, soil morphology

A PEDOLOGICAL STUDY OF SOIL GENISIS ON SKIDAWAY ISLAND

by

CHRISTOPHER P. VANAGS

B.S., The University of Georgia, 2000

A Thesis Submitted to the Graduate Faculty of The University of Georgia in Partial

Fulfillment of the Requirements for the Degree

MASTER OF SCIENCE

ATHENS, GEORGIA

2002

A PEDOLOGICAL STUDY OF SOIL GENISIS ON SKIDAWAY ISLAND

by

CHRISTOPHER P. VANAGS

Approved:

Major Professors: William Miller
David Wenner

Committee: Larry West
Ervan Garrison

Electronic Version Approved:

Maureen Grasso
Dean of the Graduate School
The University of Georgia
December 2002

For Loren

ACKNOWLEDGEMENTS

Although my name is on the front of this book-like monstrosity, indicating that I have "mastered" science, my duties mainly consisted of bringing intelligent people together and listening to what they had to say. Fortunately, I was in the right place for such a task. The University of Georgia harbors some of the best scientists around. Coupled with the fact that many are helpful and considerate individuals made my job just that much easier.

This thesis has been a group effort, and my name on the cover a misnomer. I am here as a result of my parent's unwavering encouragement. Had it not for them, I would not have the confidence to seek my life's ambition of becoming a scientist. I learned everything that I know about science from Bill Miller. He's one of those worldly people who can do anything, and still knows he's human. I admire him greatly. Like many of my major life decisions, my committee was chosen over beers at Steverino's. Dr.'s David Wenner, Larry West, and Erv Garrison have been the most helpful group of guys a kid could ask for. They exemplify the idea that science and humanity can and should coexist. If they weren't making a five-hour trip to meet me on the island, we were discussing a seminar over a beer or two. They were a tremendous influence on my life and career, and I hope to reflect their teachings in my career as a scientist.

I would also like to thank Max Schlossberg and Franz Zehetner for their guidance throughout the course of my stay here. Without their help, I never would have survived the rigors of grad school.

TABLE OF CONTENTS

LIST OF TABLES

Page

LIST OF FIGURES

CHAPTER 1

GENERAL INTRODUCTION

Sea level fluctuation during the past million years has produced drastic changes in the geomorphology of the Eastern Coast of the United States, including the deposition of a series of relict barrier islands accreted to the coast of the United States (MacNeil, 1950). The barriers appear as discontinuous ridges running parallel to the present shoreline and are commonly overlain with soils containing a humic-rich (spodic) subsoil horizon (USDA-SCS, 1974), a rarity in humid subtropical climates. It is evident that spodic horizons are currently being formed on these "new" barrier islands.

Currently, our knowledge about how spodic horizons form is unclear. Many theories exist to explain the phenomena and have been outlined by Lundström et al. (2000a). The mechanisms identified are the weathering of the base-poor parent material by high and low molecular weight organic acids, the leaching of an albic E horizon, and the deposition of a carbon-sesquioxide complex in the underlying spodic (Bh) horizon. The majority of this research has been performed in humid boreal climates, where spodosols are much more common (Buol et al., 1997).

In the subtropical Southeastern United States, spodic formation is rare due to high rates of microbial decay. And, unlike those found in Boreal climates, deposition of Fe and Al complexed with organic matter shows a strong correlation with water table depth (Tan et al., 1999; Phillips et al., 1999; Harris and Hollien, 2000). As carbon-sesquioxide complexes percolate through the soil solution and encounter the water table, the metal may precipitate, allowing the organic acids to adsorb onto the metal oxide (van Hees et al., 2000). Metal precipitation may occcur when the Al/COOH ratio exceeds the solubility constant (K_{sp}) of the oxyhydroxide (Langmuir, 1997), possibly resulting from changing the pH of the solution, evaporating the solvent, or degrading the organic acid with microbial action (Mokma and Buurman, 1982; Lundström et al., 2000b). In this environment, all three are possible due to high rates of evapotranspiration, base poor sandy soils, and high amounts of tannin-rich litter on forest floors.

Although the major factors for spodic formation are present throughout much of the barrier islands, the ubiquity of these horizons is questionable. Soil maps commonly show spodosols dominating the lower landscapes, but closer inspection reveals that spodic horizons are quite allusive, rarely producing a single developed pedon within a mapped region. Initial surveys were performed on Jekyll, Sapelo, and Skidaway Islands to find a boundary between a spodosol and an ultisol, with little luck finding a spodic pedon within a mapped unit. This quest became the underlying theme of the study, prompting a search for new methodologies to track highly variable soils such as these.

The use of geophysical survey is common in environmental research focusing on deep exploration. Here the need for subsurface imaging, where boreholes are too invasive or dangerous, has created the need for geophysical exploration. Only recently, as environmental research has begun to focus on the vadose zone, has the need for shallow subsurface exploration constituted the demand for "expensive voodoo" over traditional coring methods. This study highlights the use of ground-penetrating radar to image subsurface soil horizons, where resolution is crucial for mapping smaller areas. Although the use of ground-penetrating radar is not a widely accepted practice in soil sciences, this study aims to show that it is a viable option for mapping soil boundaries in heterogeneous environments. This can be done with minimal processing and limited knowledge of geophysical signature.

This study concentrates on identifying the major mechanisms of soil development on a Pleistocene barrier island. We've done so by characterizing a recently formed spodic horizon in association with an argillic horizon, a common association inland. A 600 m^2 plot was mapped with ground-penetrating radar, cored extensively, and geochemically analyzed to address soil genesis questions and project the future development of this association.

REFERENCES

Buol, S.W, F.D. Hole, R.J. McCracken, and R.J. Southard. 1997. Soil genesis and classification. Iowa Sate University Press, Ames, Iowa.

Harris, W.G., and K.A. Hollien. 2000. Changes across artificial E-Bh boundaries formed under simulated fluctuating water tables. Soil Sci. Soc. Am J.64:967-973.

Langmuir, D.L. 1997. Aqueous environmental geochemistry. Prentice-Hall, Inc., New Jersey.

Lundström, U.S., N. van Breemen, and D. Bain. 2000a. The podzolization process: A review. Geoderma 94:91-107.

Lundström, U.S., N. van Breemen, D.C. Bain, P.A.W. van Hees, R. Geisler, J.P. Gustafsom, H. Ilvesniemi, E. Karltun, P. -A. Melkerud, M. Olsson, G. Riise, 0. Wahlberg, A. Bergelin, K. Bishop, R. Finlay, A.G. Jongmans, T. Magmisson, H. Mamerkoski, A. Nordgren, L. Nyberg, M. Starr, L. Tau Strand. 2000b. Advances in understanding the podzolization process resulting from a multidisciplinary study of three coniferous forest soils in the Nordic Countries. Geoderma 94: 335-353.

MacNeil, F. 1950. Pleistocene shorelines in Florida and Georgia. Shorter contributions to general geology, 1949. Geol. Sur. Prof. Paper 221-F. p. 95-107.

Mokma, D.L. and P. Buurman. 1982. Podzols and podzolization in temperate regions. ISSM monograph 1, Int. Soil Museum, Wageningen.

Phillips, L.P., N.B. Comerford, D.G. Neary, and R.S. Mansell. 1999. Simulation of soil water above a water table in forested Spodosol. Soil Sci. Soc. Am. J. 53:1236-1241.

Tan, Z., W.G. Harris, and R.S. Mansell. 1999. Water table dynamics across an aquod-udult transition in the Florida Flatwoods. Soil Sci. 164:10-17.

U.S. Department of Agriculture - Soil Conservation Service. 1974. Soil survey of Bryan and Chathem Counties, Georgia. U.S. Government Printing Office, Washington, D.C.

van Hees, P.A.W, U.S. Lundström, and R. Giesler. 2000. Low molecular weight organic acids and their Al-complexes in soil solution - composition, distribution and seasonal variation in three podzolized soils. Geoderma 94:173-200.

CHAPTER 2

REVIEW OF LITERATURE

Spodosol Characteristics

Spodosols are defined by the presence of a humic-rich horizon underlying an albic eluvial layer. Although the requirements for classifying the spodic horizon differ throughout the world, Buol defines a spodic layer as “a subsurface horizon of illuvial accumulated organic matter complexed with aluminum, with or without iron” (Buol et al., 1997). The amount of organic material and the C/Al ratio varies considerably between classification systems but the accumulation of complexed organic matter and aluminum remains consistent worldwide (Mokma and Buurman, 1982). Although the definition suggests illuvation as the process for Al and organic matter accumulation, there is still a great deal of debate over the actual mechanisms behind transport and deposition of the complexes.

The podzolization process produces visually stunning profiles, where well-leached albic horizons abruptly change to dark reddish-brown as organic matter accumulates at depth. It is no wonder that Russian soil scientists were the first to conceptualize soils as a dynamic entity, altered from the surface downwards, by observing their podzol-dominated landscapes. In his theories of soil formation, Dokuchaev was the first to specify four factors, emphasizing the role of vegetation as a carbon source for illuvation (Buol et al., 1997). The history reveals some underlying generalities that soil scientists have used to conceptualize soil genesis, with illuvation playing a dominant role in subsurface formation. Although the theory works to support most pedogenic alteration, it downplays the heterogeneity associated with the parent material. This often leads to unlikely pedogenic scenarios invented to create texture contrasts, where the explanation may be a function of larger scale processes (Phillips, 2001).

Spodosol genesis has been extensively studied in colder climates, where podzolization is the most common soil forming process in the landscape (van Hees et al, 2000). Similar processes are taking place in northern Michigan, where the geology and climates are similar. In the Southeastern US, however, there are different contributing factors to forming the spodic subsoil horizon. Table 2.1 shows the dominant factors of soil formation in these two regions, contrasting the properties required for podzolization. The main differences stem from groundwater relationships and the factors required to retard microbial decay. In the case of subtropical environments, illuvation may not be as important to spodic-forming process as those in boreal regions.

Water Table Relationships

Commonly, there is a strong correlation between the parent material of a soil and the resulting water table characteristics (Jenny, 1941*)*. The significance of water table fluctuations on spodic development has recently been brought to light in the Southeastern United States (Harris and Hollien, 1999; Tan et al., 1999*)*. These studies have shown a direct correlation between water table height and depth of the spodic horizon, where, in both cases, the top of the spodic horizon was positively correlated to the top of the seasonally-fluctuation water table.

Table 2.1. Factors, diagnostic characteristics, and examples of spodosol distribution in boreal and subtropical regions

Factor	**Diagnostic characteristics**	**Boreal example**	**Subtropical example**	**References**
Parent Material	- low basic cations - low CEC - low pH - little buffering capacity	- glacial loess - fine-coarse alluvium - felsic-derived aeolian deposits	- fine-coarse alluvial sands - leached out (base poor) calcareous sediments	- Boul et al., 1997 - Chesworth, 1973
Relief	- may not form in a soil permanently saturated with water	- steeply sloping to relatively flat - no correlation with depth to water table	- gently rolling to relatively flat - strong correlation with peak of seasonally-high water table	- Harris, 2000 - Soil Survey Staff, 1975 - Phillips et al., 1999 - Tan et al., 1999
Time	Dating methods: - geomorphic interpretation - thermo-luminescence - ^{14}C on plant debris and shell material	- 150-300 yr. to develop albic E horizon - 3000+ to develop Bh (100 yrs. to decompose)	- 1000 yr. to develop E - 2000 yr. to develop Bs - 3000 yr. to develop Bh	- Burges and Drover, 1953 - Stützer, 1998
Climate	- P > ET - must leach humic acids to subsurface before decomposition occurs	- leaching from snow melt - cold temperature inhibits microbial decomposition	- high rainfall must surpass high rates of microbial decomposition	- DeConnick, 1980 - Gardner et al., 1992
Biota	- organic-rich "mohr" on surface to produce copious amounts of organic acids	spruce forests: - heath vegetation - sphagnum undergrowth	coniferous forests: - slash and long-leaf pine - palmetto and wiregrass undergrowth maritime forests: - live oak - yaupon holly - wax myrtle	- Geisler et al., 2000 - Van Breeman et al., 2000 - McKeague et al., 1982

Carbon Sources for Spodic Formation

The dominant source of carbon in the spodic horizon is humic substances. Humic substances are a "general category of naturally occurring, biogenic, heterogeneous organic substances that can generally be characterized as being yellow to black in color, of high molecular weight, and refractory" (Aiken et al., 1985). The ambiguity in this definition reflects the current knowledge of humic substances. Because speciation is not presently a reasonable option for studying these substances, little is known about the molecular make-up. Sparks (1995) provides a comprehensive review of humic substance formation, where the substances are categorized by molecular weight into humic (heavy, alkali soluble) and fulvic acids (light, alkali and acid soluble), and humin (insoluble). It should be noted, however, that the most likely model of organic acid speciation is a continuum between high and low weight molecules, not an abrupt change between the two (M.E. Sumner, personal communication, 2001). Lower molecular weight acids dissociate more readily in water and are more mobile in the soil profile, where they readily weather unstable minerals, releasing the ions into the soil solution.

Without weatherable minerals, humic substances percolate downward chelating exchangeable divalent and trivalent cations. When weatherable minerals are present, the ions released may allow the suspended solids to flocculate out of solution. Basic cations from weathered products also supply biota with enough nutrients to decompose the flocculent, releasing carbon dioxide and producing lignin (Sparks, 1995). Without available nutrients, microorganisms cannot survive long enough to break down the substances, and the substances percolate deeper into the soil profile. Harris and Hollien (2000) recreated this process in a laboratory experiment showing the formation of the carbon-rich layer beneath a bleached-out E horizon. In this experiment the podzolized soil was under a fluctuating water table. The results showed heavier Fe versus Al accumulation at depth, indicating the importance of redox potential to produce the sesquioxide layers.

Organic Matter-Sesquioxide Complexes

Debate over podzolization processes typically concerns the formation and transport of carbon-sesquioxide complexes. Mokma and Buurman (1982) suggest that Fe and Al are transported to the subsurface horizons in solution with high molecular weight organic acids. At a certain depth, this complex is precipitated when the ratio of metal to dissolved organic carbon exceeds the solubility product (K_{sp}) of the complex. Some theories suggest that the decrease in solubility results from changes in pH (van Hees et al., 2000), while others have indicated that microbial action may play a significant role in the decomposition of the organic complex (Lundström et al., 2000b; VanBreeman et al., 2000). In his theory of sesquioxide accumulation, Farmer (1980) maintains that the source of Al in the spodic layer results from the translocation of proto-imogolite substances formed in the E horizon, where particle migration accounts for the "dissolved" constituents. All of the current theories, however, suggest downward movement through the soil profile.

The general profile of a spodosol has varying amounts of organic C, Al, and Fe with depth. Although there is considerable variation in the amount of Fe present, Al always accumulates in the organic-rich Bh horizon. The profile from a typical coastal plain soil is shown (Fig. 2.1 b) to have this accumulation directly below a leached E

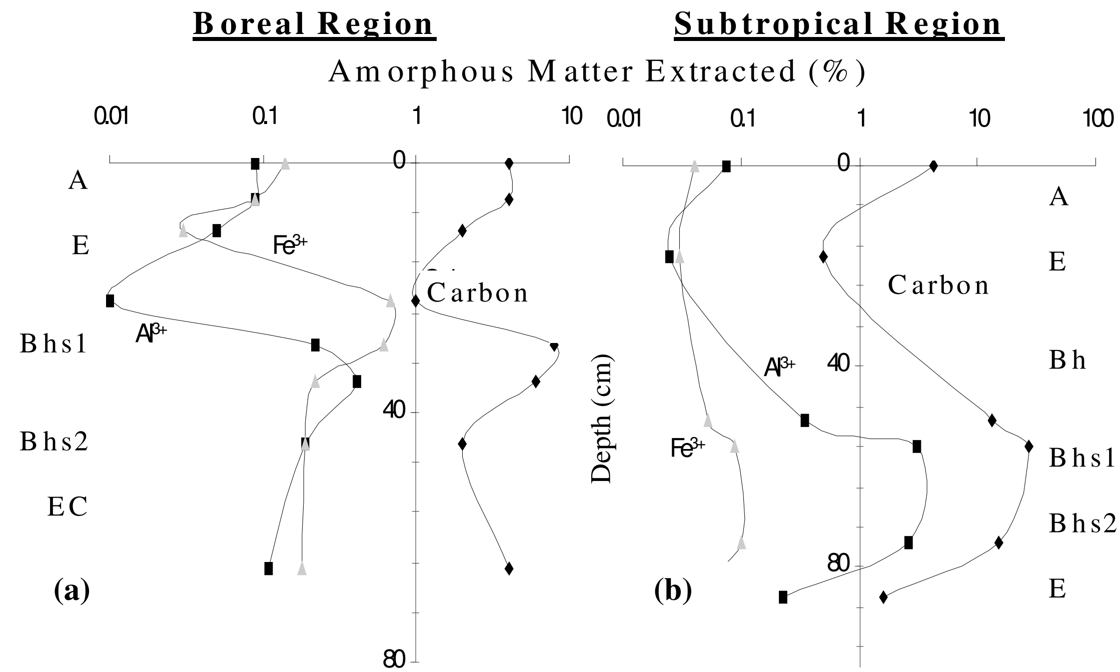

Fig. 2.1. Distribution of Al^{3+}, Fe^{3+}, and organic carbon with depth. Extractions were performed using a pyrophosphate method (Lee et al., 1988). The two profiles show an accumulation of all three constituents in the spodic (Bh) horizon. Profile a (drawn from Mokma and Buurman, 1982) shows the inflection of iron content before aluminum, whereas profile b (drawn from Lee et al., 1988) shows the inflection beneath aluminum. The subtropical profiles contain considerably less iron, likely the result of insolubility and distance from source material.

horizon. In this example, the Fe content strongly parallels the amount of amorphous Al and C. It is important to note, however, that the Fe accumulation is just below the Al, as denoted by the inflection points. This is not the case in soils formed in northern regions (Fig. 2.1 a). Small-scaled experiments on the chemical nature of this process fail to explain the source of the metals in a subtropical setting. Therefore, larger scale processes may explain this phenomenon as a function of depositional episodes associated with these coastal settings.

Soil Formation on Barrier Islands

The Eastern coast of the United States is bordered by a series of barrier islands, appearing as discontinuous sand ridges paralleling the coast, rising 1-3 m above mean sea level. The islands migrated as sea level fluctuated during the Pleistocene, arriving at their current position 4,000 yrs ago (Oertel, 1979). Island morphology changes considerably along the coast due to littoral currents, tidal fluctuations, and sediment supply (Hoyt and Henry, 1967). Much of the eastern coast is protected by wave-dominated islands, which appear as thin sandy ridges, tens to hundreds of kilometers long (Hayes, 1994). The Georgia barrier islands, however, are protected by a long gently sloping continental shelf. The shelf dissipates incoming wave energy and limits the erosive power of littoral currents. The result is large tidal fluctuations producing extensive marsh areas and incising tidal creeks in the slack-water environments landward. These barriers are shaped by a large number of migrating tidal inlets, which act to rework much of the island's periphery in relatively little time (Hoyt and Henry, 1965).

Soil formation on active barriers is limited by high energy associated with the juxtaposition of terrestrial environments with marine. Twice each day, tidal fluctuations draw millions of gallons of water landward. Solar radiation generates steady winds commonly exceeding 25km/hr, blowing offshore for half the day and onshore for the other half, with little more than an hour of rest. Storms generated thousands of miles offshore gather energy as they approach the continent and unleash their energy on the land. Sediment erosion and deposition are constantly in flux. New deposits blanket older ones, resetting soil development in the upper horizons and preserving older development below.

Directly west of the active barrier islands is a series of older ones, protected from this energy since sea level fell 40,000 yrs ago (Fig. 2.2). The Pleistocene period, characterized by its glacial episodes, produced several sets of relict barriers, now hundreds of kilometers inland, stranded during ice-age sea level regression. Since stabilization, the sediments have been pedogenetically altered. The result is well-developed subsurface horizons, which reflect the complex nature of the system that deposited them.

Skidaway Island is a Pleistocene-aged barrier island, dated at 40,000 yrs (Hoyt and Henry, 1967). Currently, it is accreting sediments on the eastern margin where it is protected from wave energy by its Holocene component, Wassaw Island. The result is the net movement of material from the western edge to the eastern edge. This process produces small, steeply cut banks exposing the Pleistocene-aged "core" of the island, identified as a spodic horizon.

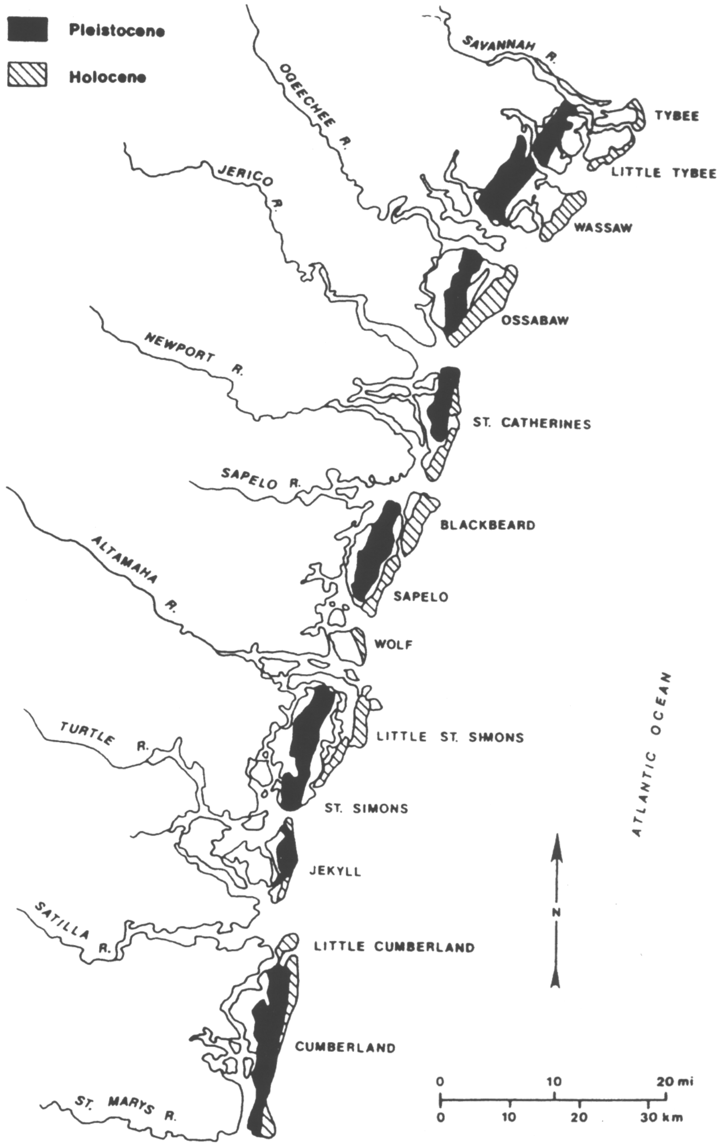

Fig. 2.2. Map of barrier islands off the coast of Georgia from Oertel (1979). Time of formation is designated by fill patterns. The map shows the actively forming Holocene islands separated by their Pleistocene components at delta mouths, where rivers originate in the Piedmont region. Away from the sediment source, the islands get progressively closer, until the Holocene component is accreted onto the stable Pleistocene island.

Using Ground-Penetrating Radar to Map Soil Horizons

Geophysicists have used ground-penetrating radar (GPR) since the early 1970s. Initially, the technology was devised to explore underground caverns and detect unexploded ordinances during the Vietnam War. In the early 1980s, scientists adapted the technology for near-surface exploration. Since that time, ground-penetrating radar has proven an accurate, cost-effective method for delineating soil horizons under most environmental conditions (Conyers and Goodman, 1997; Johnson et al., 1980).

Studies show that ground-penetrating radar reduces the average cost of a soil survey by 70% and increases human productivity per hour by 210% (Doolittle, 1987). The method generates a continuous data set along a transect, which can tie into a grid system for micro-variability studies (Collins and Doolittle, 1987). This provides an alternative to the traditional method of selective borehole measurements and is less physically demanding on the soil surveyor, provided that conditions are suitable for signal penetration and horizon delineation. Adequate signal response results from abrupt changes in the dielectric properties (discussed below). Because the efficacy of ground-penetrating radar is site specific, sites should be evaluated prior to data acquisition (Collins and Doolittle, 1987; Doolittle, 1987; Johnson et al., 1980).

Ground-penetrating radar operates by emitting electromagnetic waves into the earth. The receiver measures the reflected energy, caused by differences in the dielectric (ability to store and subsequently transmit electromagnetic energy) properties of the underlying material (Conyers and Goodman, 1997). The velocity of wave propagation is governed by the mathematical relationship:

$$V = \frac{C}{K^{1/2}} \qquad (1)$$

where:

K = relative dielectric permittivity (RDP) of the material through which the radar energy passes

C = speed of light (.2998 m/ns)

V = velocity of the radar energy as it passes through a material (m/ns)

The relative dielectric permittivity (RDP) of a material is determined by water content, particle size, elemental composition, bulk density, and temperature (Chan and Knight, 2001; Jackson et al., 1978). In general, as the material is more conductive, the electromagnetic wave is attenuated and accordingly slowed. Because the recorded signal is time-referenced, wave velocity determination is crucial to accurately interpret depth to reflections. Traditional methods of velocity determination, result in depth miscalculation by 20% or greater (Doolittle, 1987).

Values for RDPs are commonly derived in laboratories with packed columns to minimize spatial variability. The RDP is a universal standard unit, defined as the ratio of a material's electrical permittivity to the electrical permittivity of a vacuum (=1). Values for RDPs in different materials have been published extensively (Annan and Cosway, 1992; Chan and Knight, 2001; Daniels, 1996; Davis and Annan, 1989; Johnson et al., 1980,). Fig. 2.3 shows the differences in the dielectric of geologic materials and corresponding velocities, using equation 1. Typically, GPR surveys use published

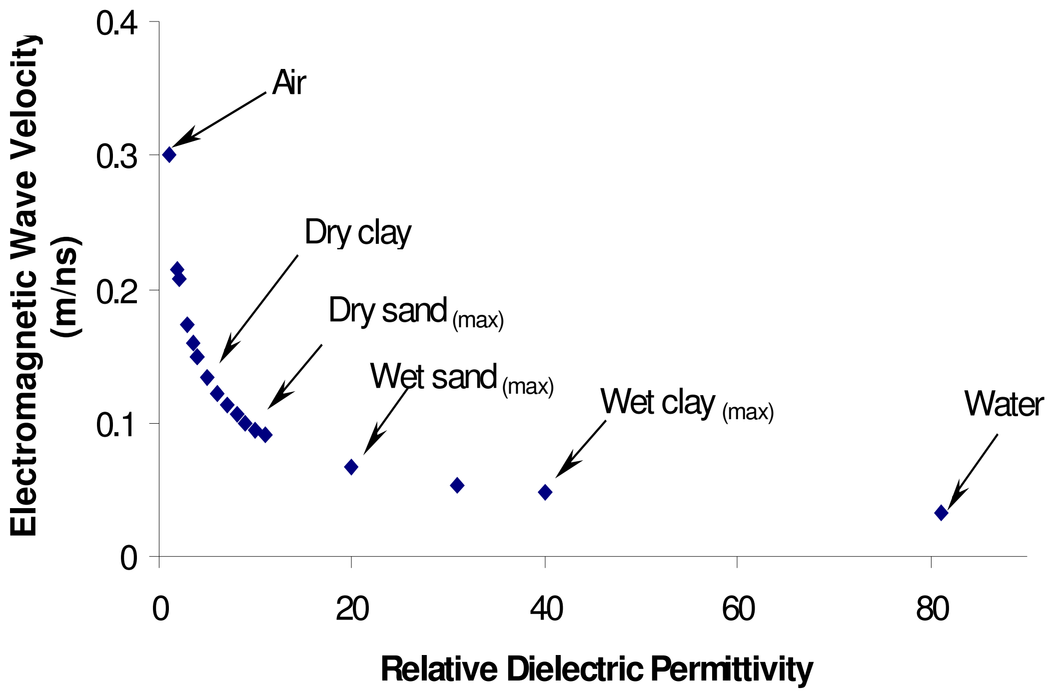

Fig. 2.3 Electromagnetic wave velocity as a function of the RDP. Maximum published values are given for particular media. Volumetric water content is commonly not reported for wet designation, so it is assumed that the maximum "wet" value is considered saturated.

values to determine the RDP for a specific site. Most surveys approximate the RDP from published values. A list of commonly accepted values is provided in Table 2.2. There are two problems with the published values. First, because of spatial soil variability, RDPs may change over the transect distance, giving false depths with each change in dielectric properties. Secondly, most published values do not account for the precise volumetric water content, the ionic strength of the solution, or the bulk density of the soil.

There are a few ways to circumvent the problems associated with published RDP values. Common midpoint stacking (CMP) has recently been used to take a "vertical sounding" of the underlying media. By increasing the distances between antenna and receiver incrementally, wave velocities are calculated by the increase in the distance that they travel. This method gives a high-resolution "snapshot" of the subsurface, resembling seismic reflection profiles. This method has been used to determine layer thickness, electromagnetic wave velocity through each reflection-generating layer, as well as water content and solute concentrations in underlying media (Boll et al., 1996; Greaves et al., 1996; Reppert et al., 2000).

As a relatively new technology, CMP is more expensive and time-consuming than traditional GPR profiling, and only covers 10 meters of a profile. The method also requires unshielded, bistatic antennae, which can separate from the receiver. Although time consuming, processing can produce accurate and repeatable estimates (GSSI, 2000) by looking at the slopes of hyperbolic reflections generated by point-source reflectors (GSSI, 2000). The slope of the line is generated by the conical geometry of the electromagnetic pulse leaving the antennae (Fig. 2.4). Reflections are generated by sources in front and behind the antennae. As the antennae approaches the reflector, the

Table 2.2. RDP's of common geologic materials from laboratory experiments.

Material	Relative Dielectric Permittivity	
	Davis and Annan, 1989	Daniels, 1996
Air	1	1
Distilled water	80	
Fresh water	80	81
Fresh water ice	3-4	4
Sea water ice		4-8
Snow		8-12
Permafrost		4-8
Sand, dry	3-5	4-6
Sand, wet	20-30	10-30
Sandstone, dry		2-3
Sandstone, wet		5-40
Limestone	4-8	
Limestone, dry		7
Limestone, wet		8
Shales	5-15	
Shale, wet		6-9
Silts	5-30	
Clays	5-40	
Clay, dry		2-6
Clay, wet		15-40
Soil, sandy dry		4-6
Soil, sandy wet		15-30
Soil, loamy dry		4-6
Soil, loamy wet		10-20
Soil, clayey dry		4-6
Soil, clayey wet		10-15
Granite	4-6	
Granite, dry		5
Granite, wet		7
Salt	5-6	4-7

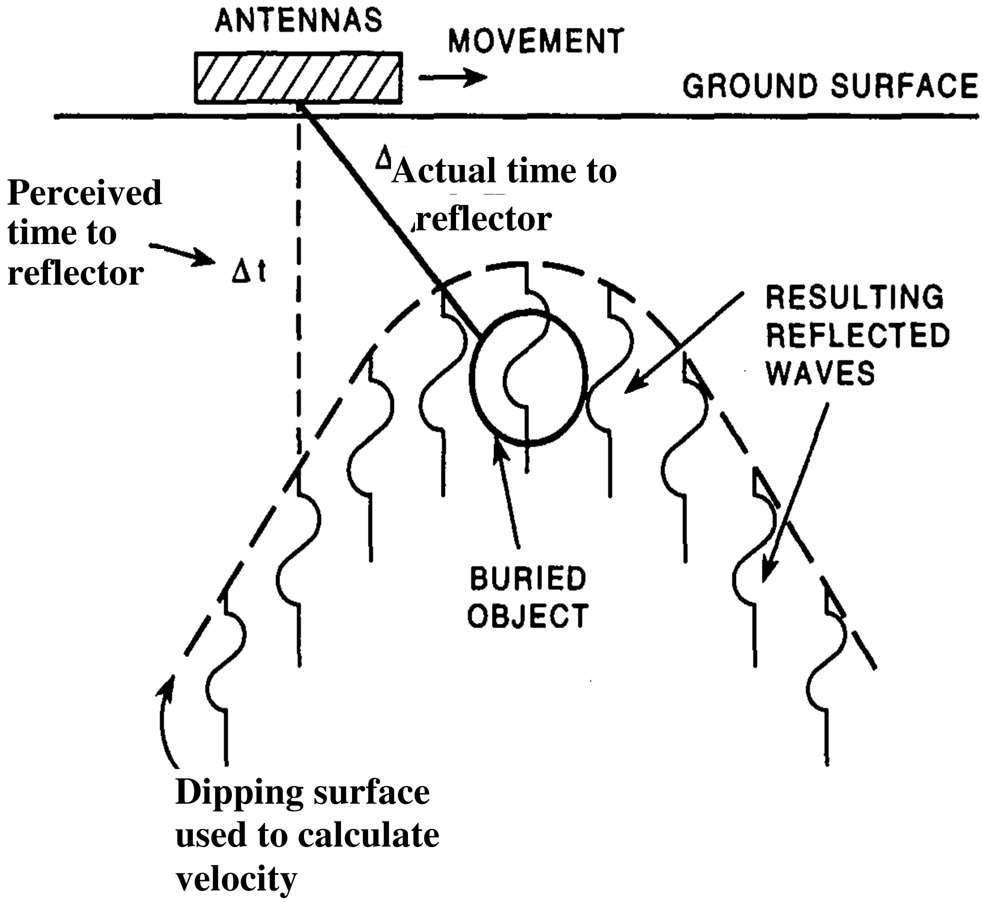

Fig. 2.4. General schematic of a GPR profile redrawn from Conyers and Goodman (1997). The figure shows the ray paths of the electromagnetic waves emitted into the ground surface, and reflected at dielectric discontinuities.

signal returns sooner until the “true” depth to reflection is achieved as the machine directly passes over the feature. This creates significant noise in the profile, but has proven useful to determine the wave velocity at any given point in a transect.

REFERENCES

Aiken, G.R., D., M. McKnight, and R.L. Wershaw. 1985. Humic substances in soil, sediments, and water. Wiley (Interscience), New York.

Annan, A.P., and S.W. Cosway. 1992. Ground-penetrating radar survey design: Proc. of the Symp. on the App. of Geophysics to Eng. and Environ. Prob. (SAGEEP).

Boll, J., R.P.G. van Rijn, K.W. Weiler, J.A. Ewen, J. Daliparthy, S.F. Herbert, and T.S. Steenhuis. 1996. Using ground-penetrating radar to detect layers in a sandy field soil. Geoderma 70:117-132.

Buol, S.W, F.D. Hole, R.J. McCracken, R.J. Southard. 1997. Soil Genesis and Classification. Iowa Sate University Press, Ames, Iowa.

Burgess, A. and D.P. Drover. 1953. The rate of podzol development in sands of the Woy district N.S.W. Aus. J. Bot. 1:83-94.

Chan, C., and R. Knight. 2001. Laboratory measurements of electromagnetic wave velocity in layered sands. Water Resour. Res. 37:1099-1105.

Chesworth, W. 1973. The parent rock effect in the genesis of soil. Geoderma 10:215-225.

Collins, M.E., and J.A. Doolittle. 1987. Using ground-penetrating radar to study soil microvariability. Soil Sci. Soc. Am. J. 51:491-493.

Conyers, L. and D. Goodman. 1997. Ground-penetrating radar-An introduction for archaeologists. Altamira Press, Walnut Creek, California.

Daniels, D.J. 1996. Surface-penetrating radar-IEE radar, sonar, navigation and avionics Series 6: London, The Institute of Electrical Engineers.

Davis, J.L. and Annan, A.P. 1989. Ground-penetrating radar for high-resolution mapping of soil and rock stratigraphy. Geophysical Prospecting 37:531-551.

DeConnick, F. 1980. Major mechanisms in formation of spodic horizons. Geoderma 24:101-123.

Doolittle, J.A., 1987. Using ground-penetrating radar to increase quality and efficiency of soil surveys. p. 11-32 *In* W.U. Reybold and G.W. Petersen (ed.) Soil sur. tech. SSSA Spec. Publ. 20. SSSA, Madison, WI.

Farmer, V.C., J.D. Russell, and M.L. Berrow. 1980. Imogolite and proto-imogolite allophane in spodic horizons: Evidence of a mobile aluminum silicate complex in podzol formation. J. Soil Sci. 31:673-684.

Gardner, L.R., B.R. Smith, W.K. Michener. 1992. Soil evolution along a forest-salt marsh transect under a regime of slowly rising sea level, southeastern United States. Geoderma 55:141-157.

Geisler, R., H. Ilvesniemi, L. Nyberg, P. van Hees, M. Starr, K. Bishop, T. Kareinen, U.S. Lundström. 2000. Distribution and mobilization of Al, Fe, and Si in three podzolic soil profiles in relation to the humus layer. Geoderma 2000:249-263.

Geophysical Survey Systems Incorporated. 2001. RADAN for Windows NT. Geophysical Survey Systems, Inc. North Salem, New Hampshire.

Greaves, R.J., D.P. Lesmes, J.M. Lee, and M.N. Toksöz. 1996. Velocity variations and water content estimated from multi-offset, ground-penetrating radar. Geophysics 61:683-695.

Harris, W.G, and K.A. Hollien. 1999. Changes in quantity and composition of crystalline clay across E-Bh boundaries of Alaquods. Soil Sci. 164:602-608.

Harris, W.G., and K.A. Hollien. 2000. Changes across artificial E-Bh boundaries formed under simulated fluctuating water tables. Soil Sci. Soc. Am. J. 64:967-973.

Hayes, M.O. 1994. The Georgia Bight barrier system. *In* Davis, R.A. (ed.) Barrier islands. Springer-Verlag, New York. pp.233-304.

Hoyt, J.H., and V.J. Henry Jr. 1965. Significance of inlet sedimentation in the recognition of ancient barrier islands. *In.* Pleistocene and Holocene sediments, Sapelo Island, Ga., and vicinity. Geol. Soc. Am. SE Sec. Field Trip 1, 1966, Guidebook.

Hoyt, J.H., and V.J. Henry Jr. 1967. Influence of island migration on barrier-island sedimentation. Geol. Soc. of Am. Bull. 78:77-86.

Jackson, P.D., D.T. Smith, and P.N. Stanford. 1978. Resistivity-porosity-particle shape relationships for marine sands. Geophysics 43:1250-1268.

Jenny, H. 1941. Factors of Soil Formation. McGraw-Hill, New York.

Johnson, R.W., R. Glaccurn, and R. Wojtansinski. 1980. Application of ground-penetrating radar to soil survey. Proc. Soil Crop Sci. Soc. Fla. 39:68-72.

Lee, F.Y., T.L. Yuan, and V.W. Carlisle. 1988. Nature of cementing materials in orstein horizons of selected Florida Spodosols: II. Soil properties and chemical form(s) of aluminum. Soil Sci. Soc. Am. J. 52:1796-1801.

Lundström, U.S., N. van Breemen, D.C. Bain, P.A.W. van Hees, R. Geisler, J.P. Gustafsom, H. Ilvesniemi, E. Karltun, P. –A. Melkerud, M. Olsson, G. Riise, O. Wahlberg, A. Bergelin, K. Bishop, R. Finlay, A.G. Jongmans, T. Magmisson, H. Mamerkoski, A. Nordgren, L. Nyberg, M. Starr, L. Tau Strand. 2000b. Advances in understanding the podzolization process resulting from a multidisciplinary study of three coniferous forest soils in the Nordic Countries. Geoderma 94: 335-353.

McKeague, J.A. 1968. Humic-fulvic acid ratio, Al, Fe, and C in pyrophosphate extracts as a criteria of A and B horizons. Can. J. Soil Sci. 48:27-35.

McKeague, J.A, F. DeConnick, and D.P. Franzmeir. 1982. Spodosols p. 216-248. *In* Wilding L.P.(ed.), Pedogenesis and Soil Taxonomy. II. Elsevier, Developments in Soil Science 11B.

Mokma, D.L. and P. Buurman. 1982. Podzols and podzolization in temperate regions. ISSM monograph 1, Int. Soil Museum, Wageningen, 126 pp.

Oertel, G.F. 1979. Barrier island development during the Holocene recession, Southeastern United States. *In* Leatherman, S.P. (ed.) Barrier islands: from the Gulf of St. Lawrence to the Gulf of Mexico. Academic Press, Inc. New York.

Phillips, J.D. 2001. Contingency and generalization in pedology, as exemplified by texture-contrast soils. Geoderma. 102:347-370.

Phillips, L.P., N.B. Comerford, D.G. Neary, and R.S. Mansell. 1999. Simulation of soil water above a water table in forested Spodosol. Soil Sci. Soc. Am. J. 53:1236-1241.

Reppert, P.M., F.D. Morgan, and M.N. Toksöz. 2000. Dielectric constant determination using ground-penetrating radar reflection coefficients. J. App. Geophys. 43:189-197.

Soil Survey Staff. 1975. Soil Taxonomy: A basic system of soil classification for making and interpreting soil surveys. USDA-SCS Agric. Handb. 436. U.S. Gov. Print. Office, Washington, DC.

Sparks, D.R. 1995. Environmental Soil Chemistry. Academic Press, Inc. San Diego, California.

Stützer, A. 1998. Early stages of podzolisation in young aeolian sediments, western Jutland. Catena 32:115-129.

Tan, Z., W.G. Harris, and R.S. Mansell. 1999. Water table dynamics across and aquod-udult transition in Florida Flatwoods. Soil Sci. 164:10-17.

van Hees, P.A.W, U.S. Lundström, and R. Giesler. 2000. Low molecular weight organic acids and their Al-complexes in soil solution – composition, distribution and seasonal variation in three podzolized soils. Geoderma 94:173-200.

Van Breemen, N., U.S. Lundström, and A.G. Jongmans. 2000. Do plants drive podzolization via rock-eating mycorrihizal fungi? Geoderma 94:163-171.

CHAPTER 3

USING GROUND-PENETRATING RADAR TO MAP SOIL BOUNDARIES IN LATERALLY-DISCONTINUOUS SOILS[1]

[1]Vanags, C.P., Miller, W.P., West, L.T., Garrison, E.G. To be submitted to *Soil Science Society of America Journal.*

ABSTRACT

A Pleistocene-aged barrier island off the coast of Savannah, Georgia was studied to identify and construct a 3-dimensional map of the boundary between a Talquin fine sand (Arenic Alaquod) and an Ocilla loamy sand variant (Umbric Paleaquult). This association is typical of soils deposited on older barriers in the Flatwoods Region, but remiss in younger, Holocene-aged sediments. Inland, a series of the relict barrier islands exist, paralleling the present shoreline, increasing in age to the west. The purpose of the study was to examine this relatively young landscape using ground-penetrating radar and identify the boundary conditions where the spodosol sharply grades to the ultisol, preempting a chronosequence study of boundary characteristics westward.

A soil boundary was studied in a 15- by 40- m grid. A high-resolution topographic map of the grid area was created using a theodelite, and the subsurface mapped with ground-penetrating radar (GPR). The sixteen, 40 m GPR transects were examined using RADAN, and compiled, producing vertical slices of reflection amplitudes with depth across the grid. The 8-10% clay increase at the soil boundary dramatically attenuated the GPR signal, resolving the boundary to within 20 cm. Localized induration of the spodic horizon produced hyperbolic reflections, confirming their discontinuous nature.

The results of this study indicate that GPR is a valuable tool for delineating soil boundaries. Changes in subsurface dielectric properties are readily identified in the field when gain parameters are set for reflections in the less attenuating media. Conservative

processing enhances the ability to identify the nature and orientation of underlying anomalies such as partial cementation.

INTRODUCTION

Skidaway Island, a Pleistocene-aged barrier island, is located 20 km east of Savannah, Georgia (Fig. 3.1). It was deposited as sea level regressed 40,000 yrs ago, exposing the island to terrestrial conditions until sea level returned 4,000 yrs ago (Hoyt and Hails, 1967). The landscape of the Flatwoods Region (SE United States) has been sculpted by sea level fluctuation, as encroaching tides erode old landscapes and deposit new ones (MacNeil, 1950; Markewich and Pavich, 1991; Markewich et al., 1987). The soils formed on these complex parent materials reflect this dynamic process. Over this region, the relict barrier islands are overlain with spodosols, ultisols and (less frequently) alfisols (USDA –NRCS, 1974). They commonly contain inclusions of contrasting textures and are laterally discontinuous in areas.

Spodosols are typically found in boreal climates. In these regions, high rates of infiltration and cold temperatures slow microbial degradation of organic acids, which are required to form the organic-rich horizon. Spodosols are more rare in subtropical zones, where they occur associated with relict barrier islands. Markewich and Pavich (1991) studied relict barriers to identify pedogenic processes concluding that the formation of spodic and argillic horizons results from separate topographically-controlled weathering pathways. Recently, others have argued that the texture contrast in the associations cannot be explained by pedogenesis, suggesting that the complexity results from heterogeneity inherent in the parent material (Gardener et al., 1992; Phillips, 2001).

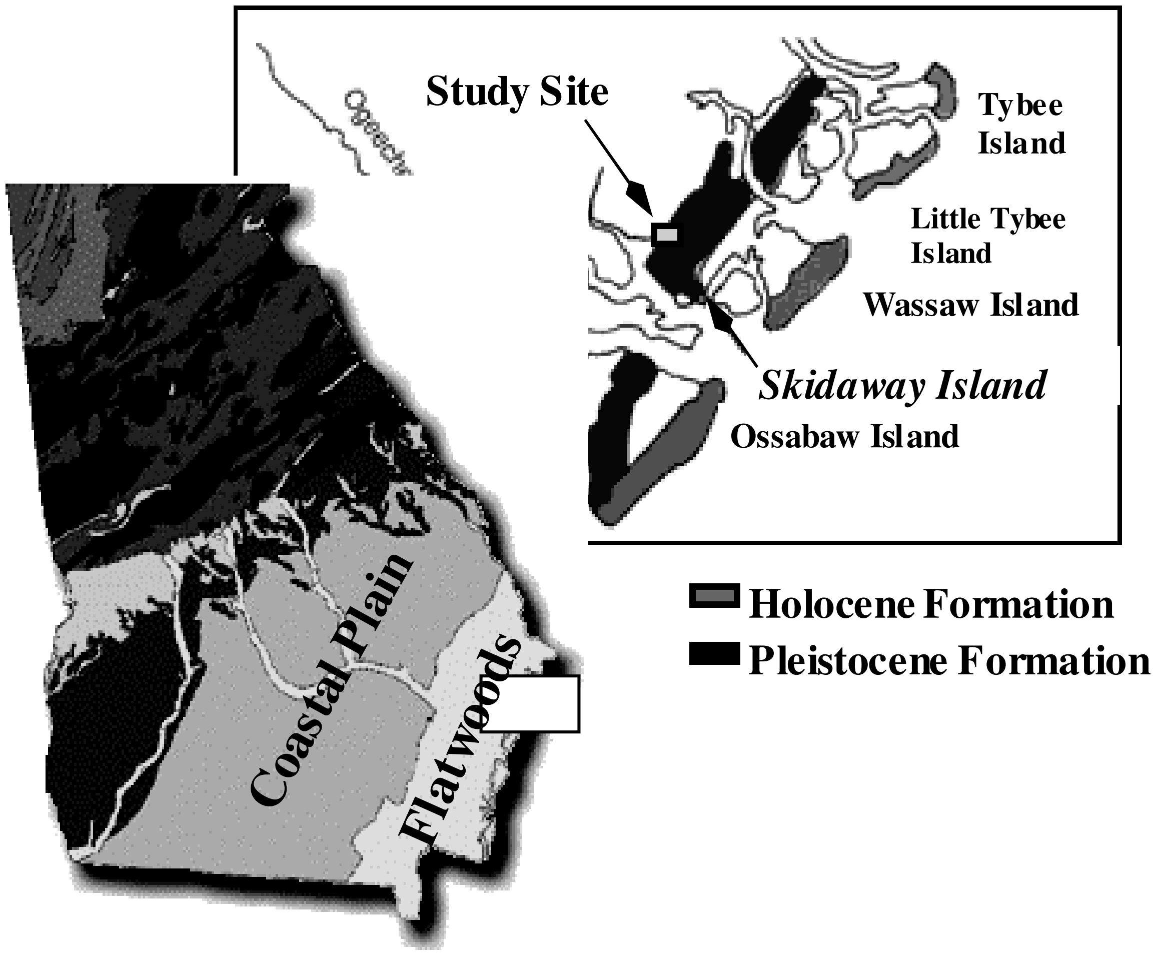

Fig. 3.1. Geologic map showing Skidaway Island relative to the Georgia coastline (http\\www.gly.uga.edu). Enlarged region shows Pleistocene-aged islands, protected by Holocene islands on the seaward edge. Coastal Plain and Flatwoods Regions labeled showing past marine deposition.

This paper highlights the use of ground-penetrating radar for mapping a soil boundary, where horizontal resolution is crucial. Geophysical surveys have become an increasingly popular method for environmental investigation due to advances in software and improvements in instrument cost and ease of use. Ground-penetrating radar significantly reduces site disturbance and produces high-resolution subsurface maps in a cost and time efficient manner (Collins and Doolittle, 1987; Doolitttle, 1982; Johnson et al., 1979). The method emits radio frequency electromagnetic pulses, which propagate downward until reflected at dielectric discontinuities in the media below. The unit continuously records the time-referenced reflections, which can be used to generate high-resolution profiles of subsurface features based on changes in dielectric properties.

OBJECTIVES

A 15- by 40-m area on Skidaway Island was studied to map the boundary characteristics of a soil association using ground-penetrating radar. This study looks at a few different processing techniques, which can be utilized to maximize the efficiency and utility of GPR surveys.

METHODS

Soil surveys were performed on Skidaway Island from December 6, 2001 through March, 2002 to identify the predominant subsurface soil horizons on the western edge of the island (Fig. 3.1). A 40- by 15- m grid was constructed with the long axis perpendicular to the identified soil boundary, using a Total Station theodelite on 1- by 1-m grid spacing. Elevations referenced to a datum were recorded to the nearest 0.1 cm. The data were plotted with Surfer (Golden Software, 1999) and interpolated with Krigging (Fig.3.2).

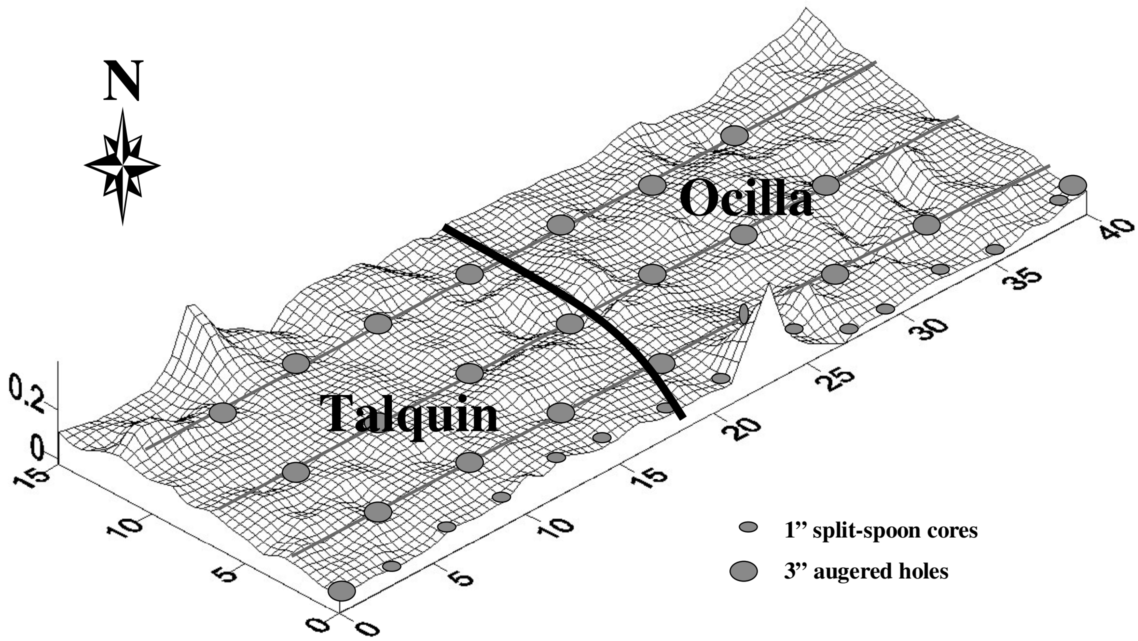

Fig. 3.2. Map of study site showing microtopographic variation. Units are meters from datum 0,0,0. Thick line represents boundary between Talquin fine sand and Ocilla loamy sand, identified by coring. Large peaks on periphery show tree crowns, slight dip associated with clay increase shown in northeastern corner of map. Circles show cores used to truth the GPR data.

Ground-penetrating radar surveys were performed on two separate occasions to track changes in profiles from moisture conditions. The first survey was performed on March 31, 2002. Following the initial survey, we cored every 3 m using a 1” split-spoon corer to a depth of 1.75 m and described the soil profiles on transect 0,0 – 0,40 with coordinates referenced to datum 0,0 (Fig. 3.2). The Munsell colors were converted to CMYK values and imported into a computer illustration package to draw the soil profiles.

On May 23, 2002, 16 GPR transects were recorded (replicating the former two), across the grid with 1 m spacing. The gain parameters were maximized for signal recovery in the sandy matrix. The GPR antenna emitted 32 scans per second, each sampled 512 times within the 60 ns window to plot reflected waveforms. The GPR transects were processed using GPR_Process (Conyers, 2002) and RADAN 3D (GSSI, 2001). The former was used to create vertical slices at depth by interpolating reflections across the grid. RADAN was used to view individual profiles to determine point-source reflectors. Individual transects were distance-normalized from user marks inserted at 1 m intervals during the survey. Following surface normalization, the wave velocity was calculated, and corrected for relief. Unprocessed files were converted to ASCI format for statistical analysis.

Following the survey, we cored three transects every 5 m with a bucket auger (7.5 cm dia.) to a depth of 1.5 m. The cores were used to identify the approximate soil boundary shown in Fig. 3.2. Horizon were separated and sealed in plastic bags for laboratory analysis. Particle size distribution was determined using the “micropipette method” (Miller and Miller, 1987). Electrical conductivity (EC) and pH were determined in a 2:1 slurry.

RESULTS and DISCUSSION

The cores used to identify the soil boundary showed an ultisol variant abruptly transitioning to a spodosol. Both profiles had umbric epipedons overlying albic horizons of varying thickness. The spodosol contained small regions of partial cementation and varied considerably in carbon content. The pH of the spodic profiles ranged from 3.5 to 4.5 and increased by 3 orders of magnitude into the Ocilla. The ultisol clay content increased 10% within 10 m.

The two GPR transects recorded at different times produced analogous profiles with reflections translated relative to changes in the moisture content. The GPR transect 0,0 – 0,40 (Fig 3.3a) clearly shows the discontinuous nature of the partially-cemented ortstien, which is identified by the hyperbolic reflections. This "noise" is generated by the conical geometry of the emitted electromagnetic energy (Conyers and Goodman, 1997), where the reflected signal reaches the receiver faster as the antenna approaches the reflector. This appears as a surface dipping away from the actual reflection source. We used the slope of this line to calculate the velocity of the electromagnetic wave (Fig. 3.3a) above the reflector.

In contrast to the hyperbolic shapes produced by the indurate spodic horizons, the leached sand and the argillic horizons produced two continuous bands of reflections, located to the right side of the profile. Both of these horizons transitioned abruptly and contained contrasting dielectric properties, which are required to produce strong reflections. The profiles show a continuous elevation for the top of the E horizon. The argillic horizon below is concave, explaining the perched water required to form the

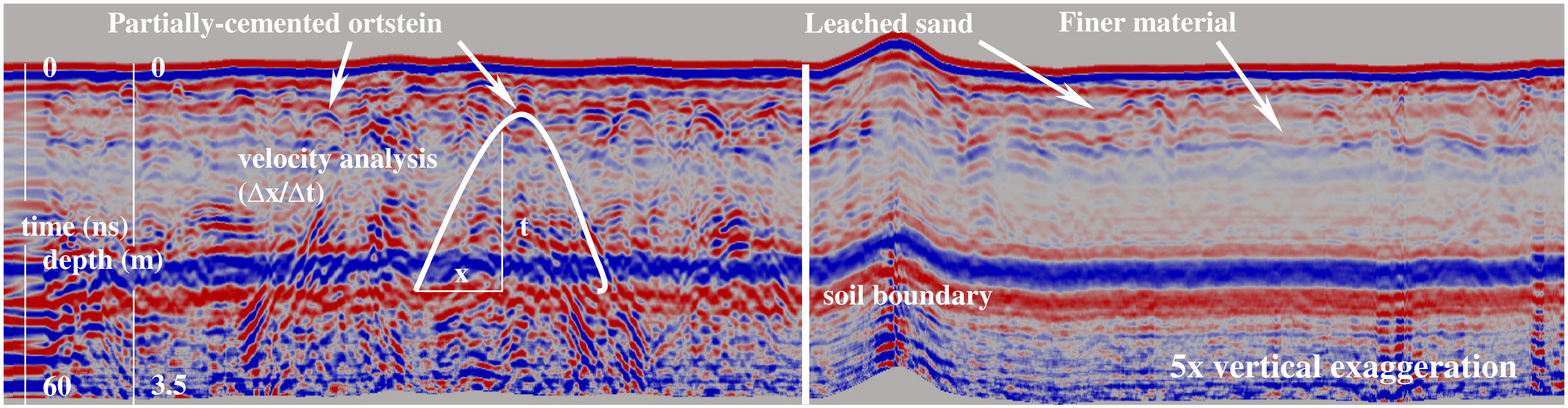

Fig. 3.3a. GPR transect 0,0 – 0,40. Transect is normalized to surface topography and laterally. Major reflections and approximate boundary are labeled. The profile is exaggerated 5x. The left side of the transect, which resembles flat layers, is a product of the distance normalization procedure, where the data was "stretched". The topographic high in middle of profile corresponds with a tree crown. The associated "bump" beneath obscured the reflections. Thick band at 2.5m is internal noise from radar.

redoximorphic features in the horizon above. Beneath the clay-rich horizons, most of the signal is attenuated, producing a “shadow”. This model was confirmed by overlaying the soil profiles generated by coring (Fig. 3.3b) on the GPR transect. The data correlated well with reflections produced by texture contrasts. The calculated dielectric, as determined by the point-source reflections, proved to adequately approximate the electromagnetic wave velocity.

The abrupt change in subsurface material is evident in profiles where a shadow is produced below the material. However, the precise location of the transition was difficult to locate and trace from one transect to the next. To improve the horizontal resolution, transects were compiled and converted to x,y,z format, where the x and y variables correspond to the grid coordinates and the z to the mean amplitude of reflection at specified depth intervals. The process produced slice maps showing reflection amplitudes at given depth using a surface mapping program. Fig. 3.4 shows slice maps of the grid at 10 ns intervals. The image maps clearly delineate the boundary to within 20 cm. Each slice averages 10 ns of reflection amplitude data, producing 6 slices.

The vertical resolution for slice maps is limited by the frequency of the electromagnetic waves, such that a slice must encompass an entire cycle of a wavelet (Conyers, pers. comm.). Because the slices are time-referenced, a dielectric constant must be specified to determine exact depth. In this case, the dielectric varied between 5.8 and 8.7 throughout the profiles due to changes in moisture content. This caused a 20% variation from the mean elevation, indicating that this method is limited in the vertical

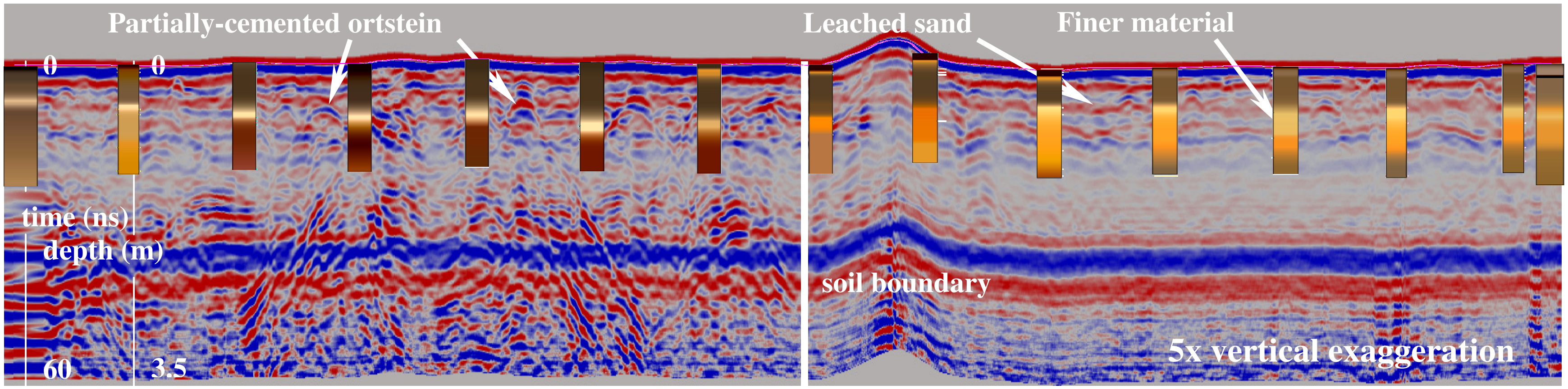

Fig. 3.3b. Profile drawn from cores of transect 0,0 – 0,40. The vertical scales are correlated based on a continuous dielectric, calculated from the point-source reflections. Borehole diameters not to scale, but are relative to area observed (thick profiles represent augered holes). Colors were converted from Munsell to CMYK using Munsell conversion software. Horizon boundaries are drawn to represent depth and gradient between colors as noted in the field.

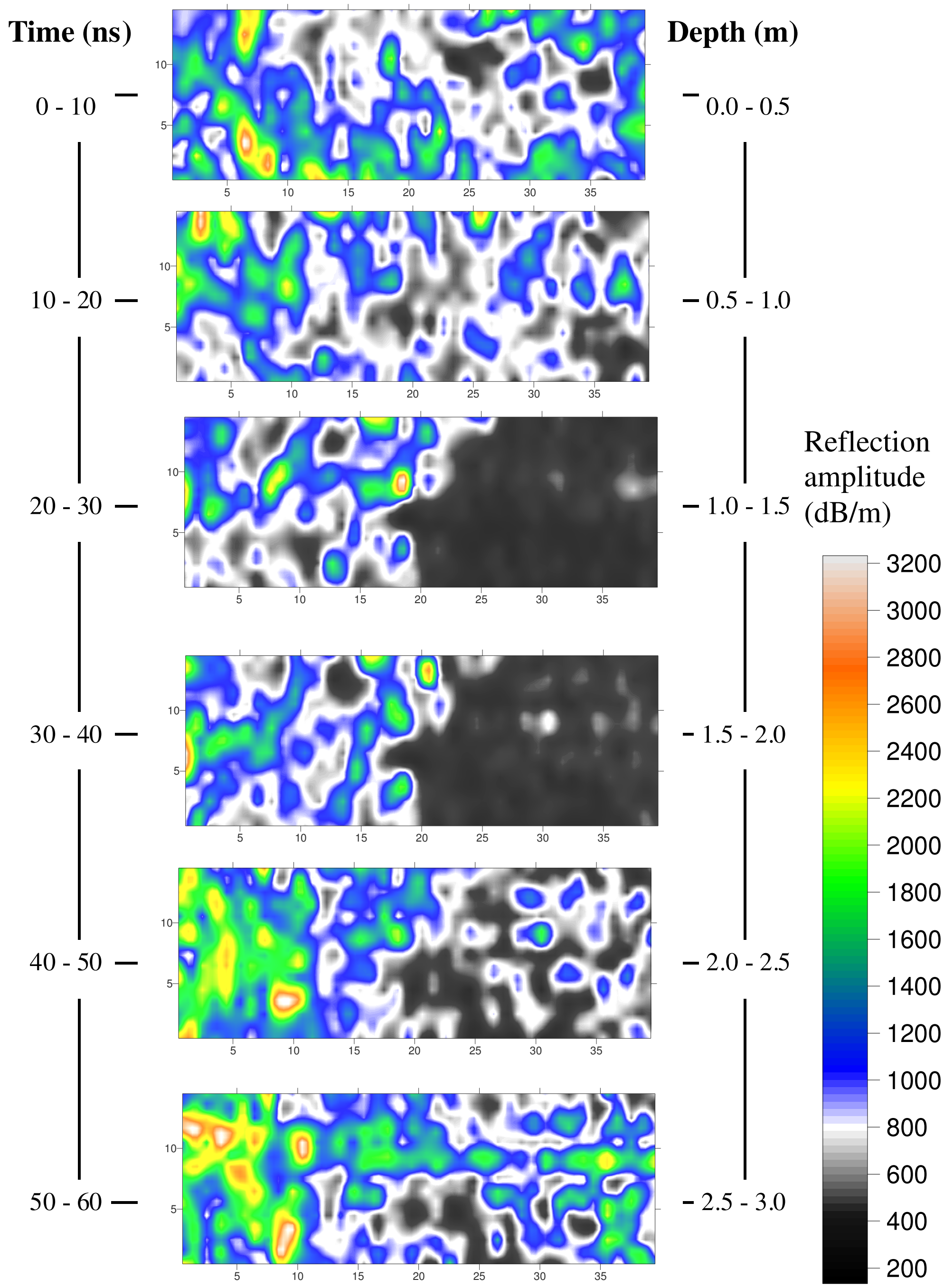

Figure 3.4. Slice maps showing the relative difference in amplitude reflections with depth. Axis labels show time signature and depth (converted using the dielectric constant). It is important to note that the depth is +/- 20% based on the relative changes in the dielectric across the grid.

direction by changes in moisture conditions across the grid. Viewed individually, the profiles compensate for lateral changes in dielectric properties using variable velocity migration from multiple point-source reflectors.

CONCLUSIONS

The increase in clay dramatically attenuated the GPR signal, enabling us to see the soil boundary in the field while profiling. The difference was accentuated by setting the gain parameters to maximize signal recovery in the less conductive media. Although the individual profiles reflected this change, slicing the data clearly improved the interpretability of the GPR data to reference the lateral extent of the attenuating media (in this case, the agrillic horizon). The partially-indurated ortstein layer produced point-source reflections, which were visible on profile maps and used to calculate the electromagnetic wave velocity to correctly identify the depth of the reflectors.

The two processing techniques worked well to compliment each other. The individual transects provided a way to calculate electromagnetic wave velocity. Profile analysis allows the user to accurately calculate depth to reflection using velocity migration. Standing alone, this process makes it difficult to determine the lateral extent of the argillic horizon over the grid. By slicing the data, the user may generate contour maps of reflection amplitudes at specific depths (relative to the vertical resolution), showing lateral differences in reflection amplitudes. In this environment, it resolved a soil boundary to +/- 20 cm, indicating that the boundary was laterally-discontinuous. The vertical resolution is limited for time slice analysis due to wave-form averaging and dielectric variation across profiles.

This type of environment was ideal for GPR, representing a “best case” scenario, due to dramatic changes in dielectric properties of the soil horizons. It should be noted that this case only exists in depositional environments or where pedogenic development has produced abrupt changes in the soil dielectric. The use of GPR is limited to these types of environments based on the fundamental properties of electromagnetic reflection, which are a function of the change in dielectric and the distance that the change occurs over.

REFERENCES

Collins, M.E., and J.A. Doolittle. 1987. Using ground-penetrating radar to study soil microvariability. Soil Sci. Soc. Am. J. 51:491-493.

Conyers, L. 2002. Manual for GPR_Process.

Conyers, L., and D. Goodman. 1997. Ground-penetrating radar - an introduction for archaeologists. Altamira Press. Walnut Creek, California.

Doolittle, J.A. 1982. Characterizing soil map units with the ground-penetrating radar. Soil Sur. Hor. 23(4):3-10.

Gardner, L.R., B.R. Smith, W.K. Michener. 1992. Soil evolution along a forest-salt marsh transect under a regime of slowly rising sea level, southeastern United States. Geoderma 55:141-157.

Geophysical Survey Systems Incorporated. 2001. RADAN for Windows NT. Geophysical Survey Systems, Inc. North Salem, New Hampshire.

Golden Software, Inc. 2000. Surfer 7. Golden Software, Inc., Golden Colorado.

Hoyt, J.H., and J.R. Hails. 1967. Pleistocene shoreline sediments in coastal Georgia; deposition and modification. Science 3769:1541-1543.

Johnson, R.W., R. Glaccurn, and R. Wojtansinski. 1979. Application of ground-penetrating radar to soil survey. Proc. Soil Crop Sci. Soc. Fla. 39:68-72.

MacNeil, F. 1950. Pleistocene shorelines in Florida and Georgia. Shorter contributions to general geology, 1949. Geol. Sur. Prof. Paper 221-F. p. 95-107.

Markewich, H.W., M.J. Pavich, M.J. Mausbach, B.N. Stuckey, R.G Johnson, and V.M. Maryland Gonzalex. 1987. Age relations between soils and geology in the Coastal Plain of and Virginia. U.S. Geol. Sur. Bull. 1589A:34 pp.

Markewich H.W., and M.J. Pavich. 1991. Soil chronosequence studies in temperate to subtropical, low-latitude, low-relief terrain with data from the eastern United States. Geoderma 51:213-239.

Miller, W.P. and D.M. Miller. 1987. A micro-pipette method for soil mechanical analysis. Comm. in Soil Sci. Plant Anal. 18:1-15.

Phillips, J.D. 2001. Contingency and generalization in pedology, as exemplified by texture-contrast soils. Geoderma. 102:347-370.

U.S. Department of Agriculture – Soil Conservation Service. 1974. Soil survey of Bryan and Chathem Counties, Georgia. U.S. Government Printing Office, Washington, D.C.

CHAPTER 4

BOUNDARY CHARACTERISTICS OF A SPODOSOL/ULTISOL ASSOCIATION ON A PLEISTOCENE BARRIER ISLAND[2]

[2]Vanags, C.P., Miller, W.P., West, L.T., Wenner, D.B. To be submitted to *Geoderma*

ABSTRACT

The Flatwoods Region of the Southeastern United States contains relict barrier islands, which were deposited during the Pleistocene. The soils associated with these deposits are heterogeneous and commonly contain abrupt textural transitions and intermittent development. The complexity of these soils raises questions of pedogenic development in relation to the high-energy environment where they were initially deposited. This paper aims at characterizing a laterally discontinuous soil association commonly found in the Flatwoods Region to better understand pedogenic processes in heterogeneous parent material. A 40,000 yr old barrier island was chosen to represent the earliest point where this soil association can be found in the Southeastern United States.

Using ground-penetrating radar, we identified a soil transition on the western edge of Skidaway Island. A 40- by 15- m grid was constructed perpendicular to the boundary and microtopography mapped with a theodelite. Three transects were cored on five meter intervals, and one on three meters. Particle size distribution, gravitational water content, electrical conductivity (EC), and pH were determined for each horizon sampled. Six selected profiles were analyzed for exchangeable and soluble Al, Ca, Mg, K, and Na as well as total C, N, and S.

The two soils were classified as Talquin fine sand (uMBRIC Alaquod) and a variant of an Ocilla loamy sand (Umbric Paleaquult). The microtopography shows a shallow depression associated with the Ocilla complex. The abrupt boundary and weakly developed structure in the Ocilla, suggests that the subsurface horizon was a result of deposition. High soluble cation concentrations show saltwater influence at depth, which

correlate with the top of the spodic horizon. This suggests that the carbon-rich material may have precipitated as a result of flocculation.

INTRODUCTION

Coastal Plain pedogenesis is difficult to interpret, due to complex soil associations in the area. Many suggest that the textural contrasts have resulted from diverging soil formation pathways (Ciolkosz et al., 1989; Markewich and Pavich, 1987). Recent studies, however, claim that formation pathways do not fully explain the heterogeneity in these environments. They suggest that the majority of differences result from complex deposition rather than pedogenic processes (Gardner et al., 1992; Phillips et al., 1996; Phillips, 2001).

Pleistocene sea level fluctuations have reworked sediment on terrestrial margins. These high-energy environments continually redistribute material as seawater encroaches on the land, tidal creeks and inlets migrate, and storms carry sand across the breadth of the islands (Davis, 1992; Gardner et al., 1992; Hoyt and Henry, 1967). Highly variable soils in the Coastal Plain reflect this complex depositional history, where spodosols and ultisols are commonly adjacent to one another. In Boreal regions, where spodosols are much more extensive, this soil association is rare, and there is little dependence on water table fluctuations. The mechanism for spodic formation is under considerable debate in the Coastal Plain region due to their sporadic presence, dependence on water table fluctuations, and their common association with argillic horizons.

OBJECTIVES

Skidaway is a 40,000 yr old barrier island located off the coast of Georgia (Fig. 4.1). Protected by its Holocene-aged component (Fig 4.2), it has remained relatively

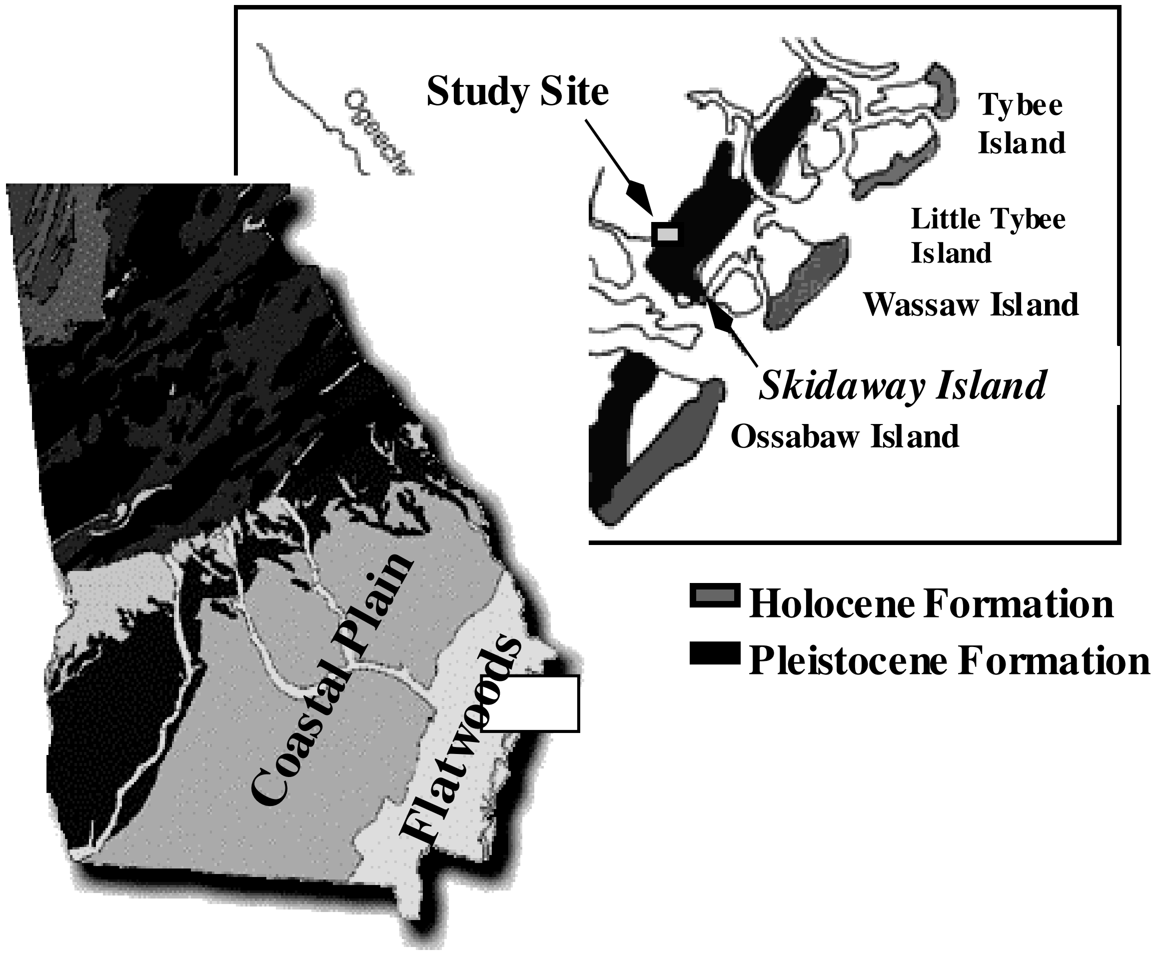

Fig 4.1. Geologic map showing Skidaway Island relative to the Georgia coastline). Enlarged region shows Pleistocene-aged islands, protected by Holocene islands on the seaward edge. Coastal Plain and Flatwoods Regions labeled showing past marine deposition (redrawn from http\\www.gly.uga.edu Jan. 2002).

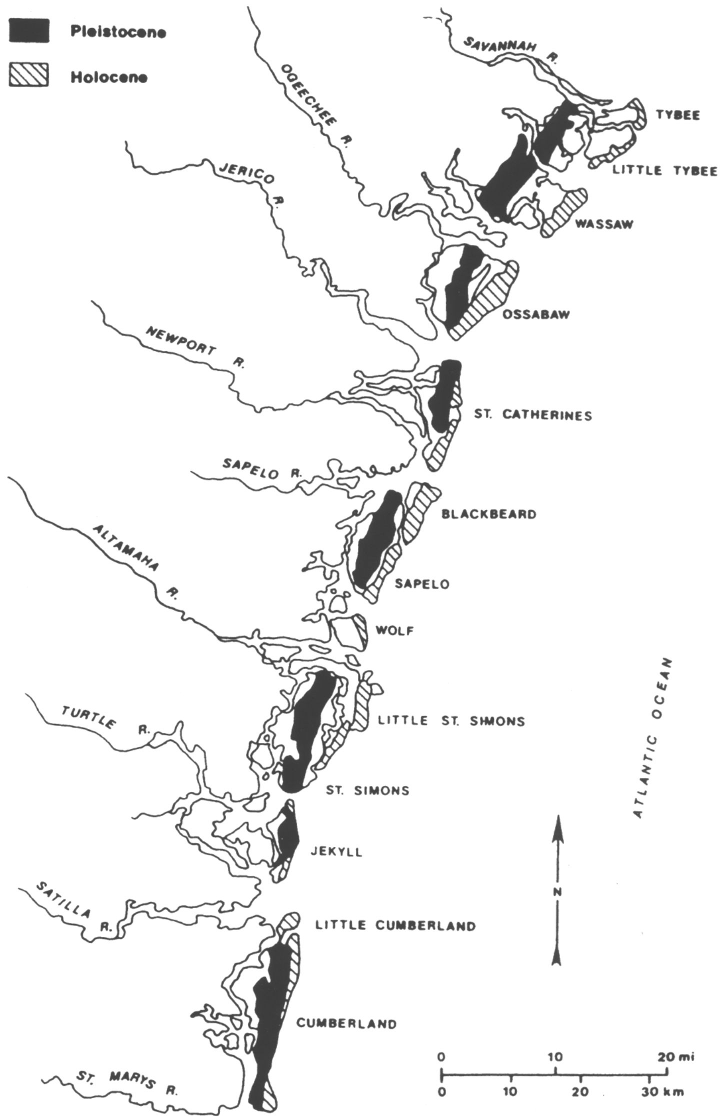

Fig. 4.2. Map of barrier islands off the coast of Georgia. Time of formation is designated by fill patterns (Oertel, 1979).

stable, allowing for pedogenic development to occur (Hoyt and Hails, 1967). This study aims to characterize a boundary between soils with contrasting subsurface horizons in hopes of identifying the dominant factors for soil development.

SITE DESCRIPTION

The study site is located on the western-most portion of Skidaway Island within Skidaway Island State Park (Fig. 4.1). It is located at the edge of a maritime climax forest, approximately 150 m from the marsh transition to the intercoastal waterway. The grid encompassed two distinctly different vegetation regimes, which reflect the soil boundary.

The more eastern (upland) areas are underlain by spodic soils. Vegetation is dominated by loblolly pines (*Pinus tieda*) and live and water oaks (*Quercus virginiana, Quercus nigra),* with interspersed red bay (*Persea borbonia*) and yaupon holly (*Ilex vomitoria*), containing little understory. Comprised, mostly, of partially decomposed pine needles, the O horizon was typically 2- to 5- cm thick. The areas that contain finer textured soils are overlain with cabbage palm (*Sabal palmetto)* and saw-palmetto (*Serenoa repens*) and the understory is covered in thick bunch grasses. These soils contained significantly thinner O horizons (absent in many areas) revealing that moles, wild boar, and large ant colonies had disturbed much of the topsoil. Commonly, there were hardened clay balls (< 1 cm diameter) mixed in with the upper 10 cm of the soil. The entire south end of the island is mapped as Leon fine sand (Aeric Alaquod) and Ellabelle loamy sand (Aerinic Paleaquult).

METHODS

Soil surveys were performed on Skidaway Island from December 6, 2001 through March, 2002 to identify the predominant subsurface soil horizons on the western edge of the island. A soil boundary was identified and a 40- by 15- m grid was constructed with the long axis perpendicular to the boundary. Elevations were recorded to the nearest 0.1 cm using a Total Station theodelite on 1- by 1- m grid spacing. Elevations were plotted with Surfer (Golden Software, 2000) and interpolated with Krigging (fig.4.3).

Four complete transects were cored for visual inspection and laboratory analysis. Transect 0,0 – 0,40 (referenced to 0,0 in Fig. 4.3) was cored on 3 m intervals using a split-spoon corer to a depth of 1.5 m. Each profile was described and returned to the hole. Later, three transects were augered on 5 m intervals with a bucket auger (7.5 cm dia.) to a depth of 1.75 m (Fig. 4.3). The samples were placed in troughs, described, and sealed in plastic bags.

Particle size distribution was determined using the "micropipette" method (Miller and Miller, 1987). Organic rich horizons were treated with H_2O_2 and the pH was adjusted with NaOH prior to dispersion. Sand size fractions were determined by dry sieving. Gravitational moisture content was determined by oven-drying 40g samples at 50C° and recording water loss. Electrical conductivity (EC) and pH were determined for all samples in a 2:1 slurry using electrodes.

The cation exchange capacity was determined by summing the major exchangeable cations extracted with 0.2M $BaCl_2$ (Sumner and Miller, 1996). Carbonate-containing horizons were extracted with 0.1M NaCl for Ca determination, to prevent

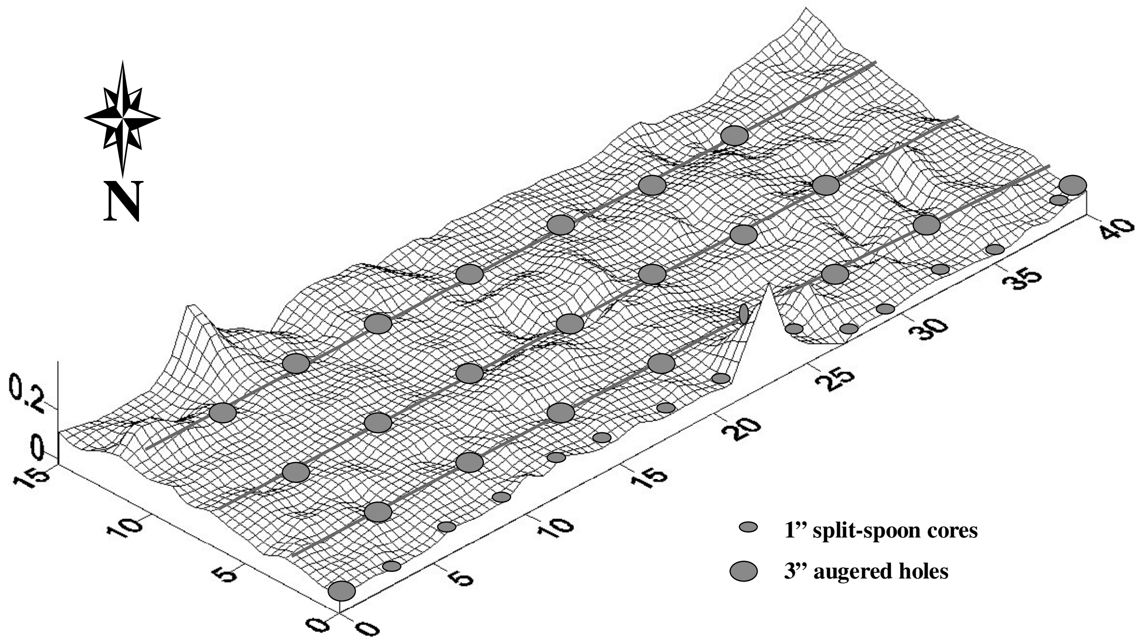

Fig 4.3. Sampling schematic of study site. Exaggerated 10x showing microtopographic variation of the study site, which contained no perceivable slope. Mounds on periphery show tree crowns. Units are meters from datum 0,0,0.

carbonate dissolution. Concentrations of Ca, Mg, Na, and K were measured with an atomic absorption spectrometer (AAS) and Al was determined using inductively coupled plasma mass spectrometry (ICP-MS). Soluble salts were subtracted from the CEC measurements, where contributing cations were estimated by 2:1 DI extraction (Rhoades, 1996). Total C, N and S were determined by dry combustion on finely-ground samples with a LECO 2000 CNS analyzer.

RESULTS AND DISCUSSION

Extensive coring revealed that the majority of soils around the island either lacked a diagnostic subsurface horizon or were weakly developed. The mapped boundary was identified by the shift in vegetation, however, the profiles did not meet the taxonomic criteria for the mapped soils. The soils were reclassified as Talquin and Ocilla due to the presence of umbric epipedons. The Ocilla was termed a “variant” due to high base saturation, assumed to be the result of shelly material present on the site (Table 4.1).

Although the Ocilla met the general criteria for an argillic horizon, the weakly developed structure and abruptness of the clay increase suggested that the horizon was not formed by clay translocation as the taxonomy suggests. An extensive microdepression corresponded to the soil boundary (Fig 4.4). It is plausible that the depression resulted from the compaction of the clay-rich horizon in the Ocilla.

The profile descriptions show appreciable amounts of clay in the surface horizons (8 - 25%), which are unaccounted for in the taxonomic class of the soil. This was the result of common clay nodules mixed into the surface horizon. These features may have

Table 4.1. Selected properties of typical profiles found within the mapped regions

	Horizon	cm Depth	Munsell color	% Sand	% Silt	% Clay	% MS/FS	% BS
Talquin fine sand	A1	0 – 10	Black "salt-n-pepper" (2.5Y 2.5/1)	70.7	9.8	16.8	0.10	54
	A2	10 – 28	Dark brownish gray (10YR 3/2)	85.2	6.1	5.0	0.09	28
	E/Bw	28 – 53	Dark yellowish brown (10YR 4/4)	85.6	5.9	5.7	0.10	24
	E	53 – 79	Light yellowish brown (2.5YR 6/2)	87.4	5.0	3.2	0.09	26
	Bh1	79 – 91	Very dark brown (10YR 2/2)	84.4	4.6	8.2	0.09	21
	Bh2	91 – 137	Reddish brown (5YR 4/4)	86.1	5.1	6.4	0.10	59
	Bhs	137 – 165+	Reddish brown (5YR 4/4)	92.4	2.3	2.6	0.19	57
Ocilla loamy sand	A1	0- 10	Very dark brown (2.5Y 2.5/1)	67.1	9.6	16.6	0.10	99
	A2	10 - 20	Dark brownish gray (10YR 3/2)	76.9	21.0	0.6	0.11	100
	E	20 - 33	Light yellowish brown (2.5YR 6/2)	84.7	7.8	5.0	0.12	100
	Bt	33 - 114	Brownish yellow (10 YR 6/6)	74.4	6.3	19.4	0.14	100
	C	114 –165	Grayish brown (10 YR 5/2)	87.9	3.7	10.4	0.18	100

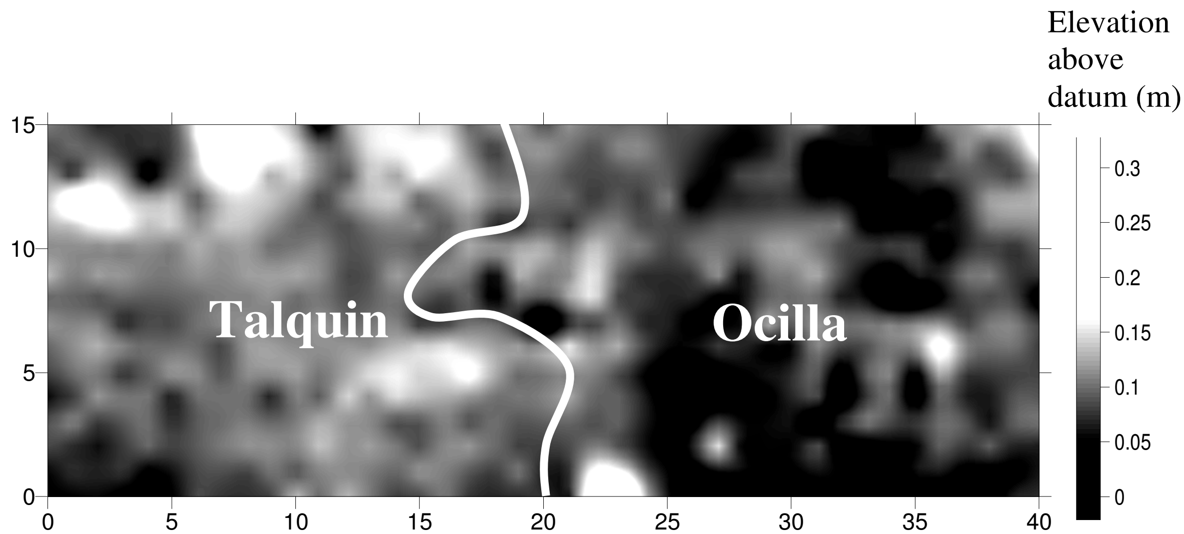

Fig 4.4. Image map of elevation data showing large microdepression associated with the soil boundary. Boundary shown was mapped using ground-penetrating radar. There is no perceivable slope on the site.

resulted from a tidally-driven washover event, where entrained marsh mud was deposited on the surface. This is reflected by a highly conductive epipedon and the occasional presence of clay-rich histic layers (3- to 10- cm thick) 4 cm below the surface, in the Ocilla complex.

The particle size distribution at depth varied across the grid, showing a maximum clay increase of 10% across the soil boundary (Fig. 4.5). Within the Ocilla complex, clay content increased 5-10% with depth, transitioning abruptly beneath a well-leached E horizon. The argillic layer varied from 30 to 60 cm thick, increasing in thickness towards the boundary, then pinching out sharply (Fig 4.6). A saturated brownish gray fine sand was found below the argillic. Above the argillic horizon was a well leached E horizon, which contained plinthite at the surface. The top of the E horizon remained at a constant level throughout the profiles. The morphology of the horizon and reticulate modeling within the argillic suggests that the horizon formed as a result of redox conditions, whereby Fe was reduced and mobilized during periods of saturation.

In the Talquin, clay content increased from 2- to 5% with depth. This profile also had a well-leached E horizon, which gradually transitioned to the spodic. Unlike the Ocilla complex, the top of the E paralleled the spodic horizon. The thickness of the horizon remained relatively constant, and pinched out at the soil boundary (Fig 4.6).

The spodic horizon in the Talquin contained strong subangular blocky structure in parts. The sporadic presence did not show any trends relating to the soil boundary. When present, the cemented portion of the spodic occurred on top, and gradually graded to single-grained structure. The horizon was lighter and had a reddish hue. The spodic layer loosely paralleled the top of the observed water table. The lateral continuity was

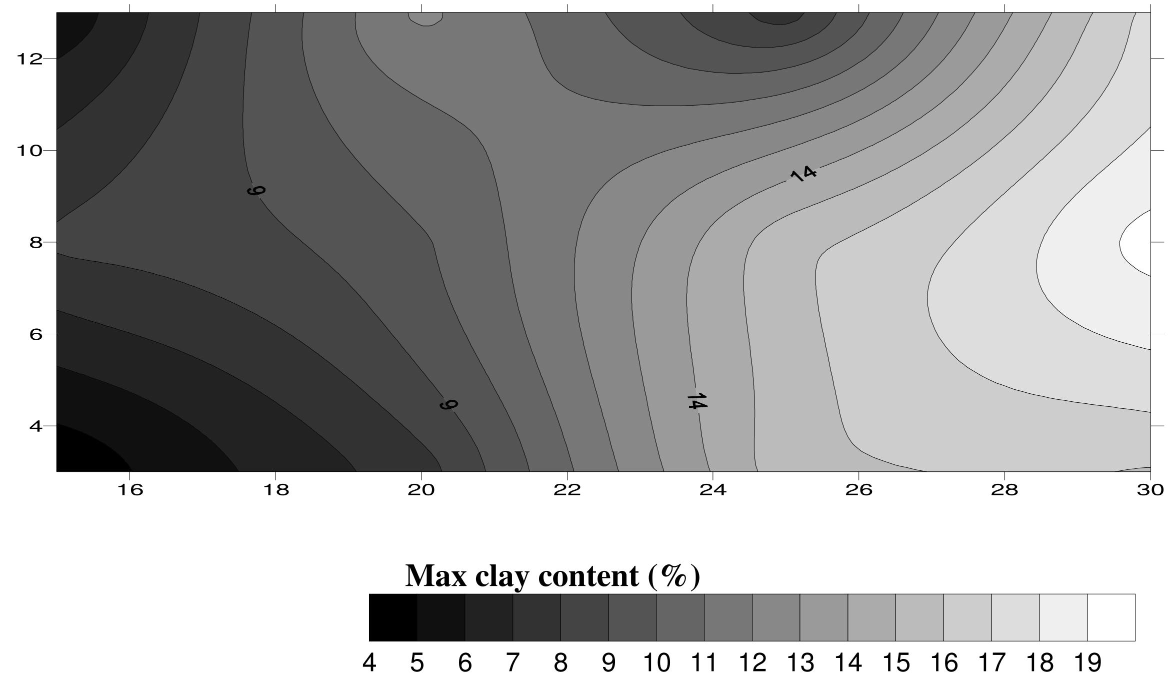

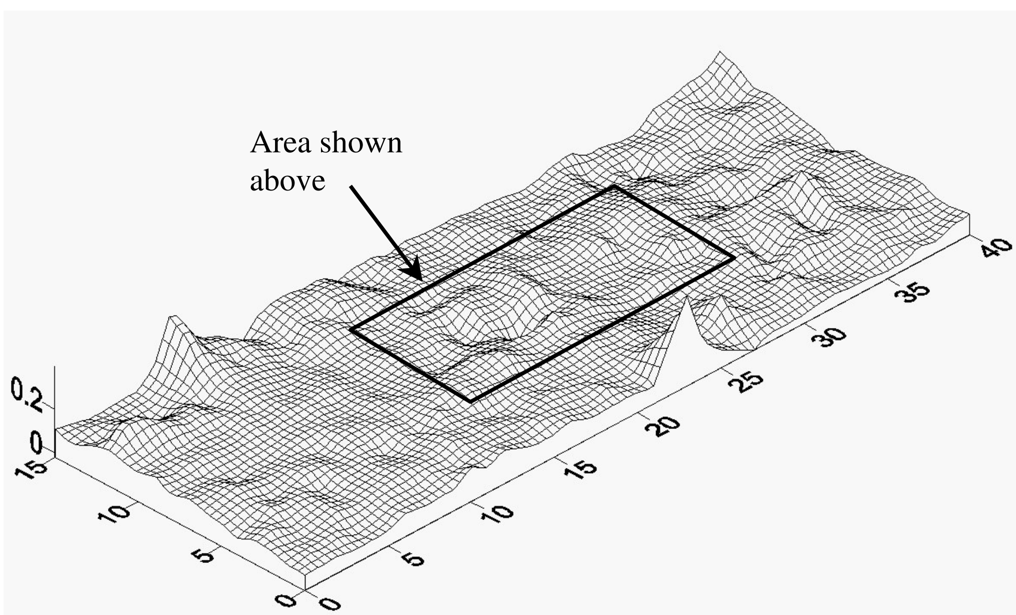

Fig 4.5. Maximum clay content for profiles over a selected portion of the grid (shown in figure below). Contour lines show clay content of the subsurface horizon as the Ocilla grades into the Talquin. Contour interval represents 1% clay content.

Transect 0,0 – 0,40

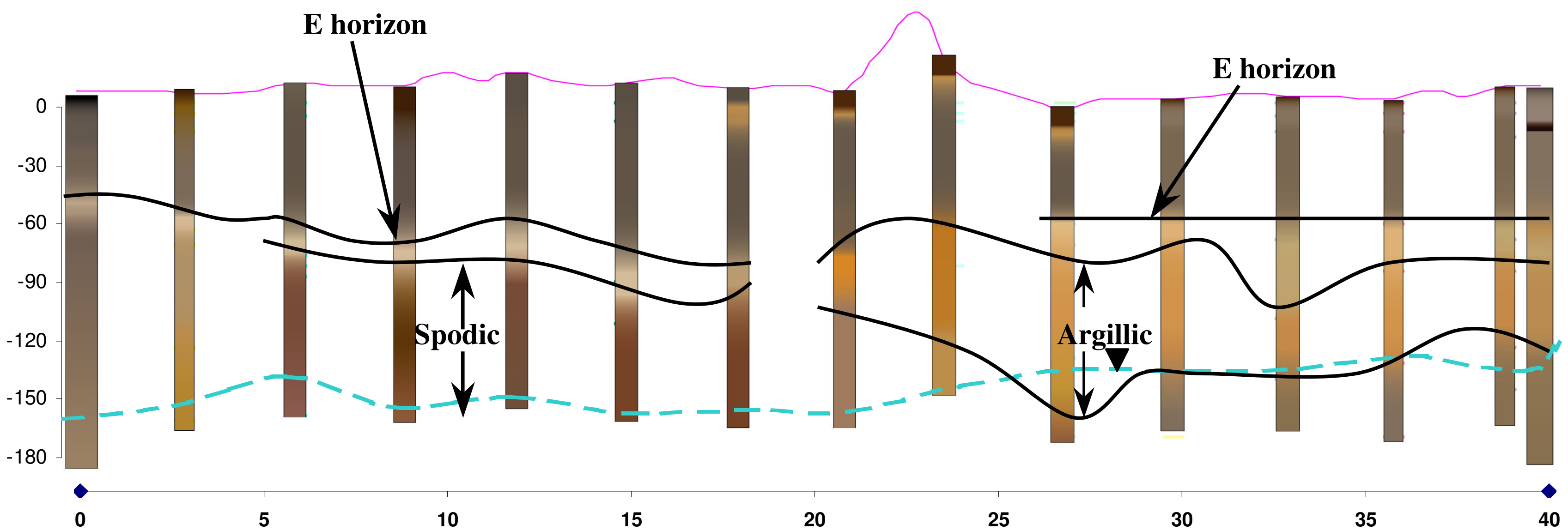

Fig. 4.6. Transect 0,0 – 0,40 showing cross section of subsurface horizons. Vertical scale is exaggerated 5x. Profiles were scaled relative to topography (shown in pink). Colors were converted from Munsell to CMYK values. Horizons are labeled according to field observations. The water table (shown as blue dashed lines) is delineated by observation at time of coring.

unclear but studies of this association show the spodic horizon curving upward into the A horizon of the adjacent ultisol (Tan et al., 1999).

The ratio of medium sand to fine sand was plotted vs. depth to determine variation in coarse grain size (Fig. 4.7). Shaw and Rabenhorst (1999) used this method to show differences in parent material in coastal plain settings. Due to its relative insolubility, quartz sand should reflect the texture of the parent material when plotted as a percentage of the total sand fraction. The material is dominated by the fine sand fraction with medium sand as the next common size. The coarser sands at depth indicate a different depositional episode. Analysis of variance (ANOVA) and Student t-test for unequal variances showed a significant difference in the mean sediment size ($p<0.00005$), indicating differences in depositional energy.

The depth to the discontinuity appears to correlate with the upper boundary of many of the subsurface horizons (Fig 4.6). The indurated portions of the spodic horizon associated with this layer lose structure at this depth but retain their organic matter coatings.

The soil profiles had dramatically different chemical properties, reflected by the abrupt change in vegetation across the boundary. The pH ranged from 3.5 to 8.2 at equal elevations across the boundary (Fig 4.8). Profiles showing the pH ranges at depth across the three transects indicate that dissolution at the boundary occurs laterally over 15 m, where the hydrogen concentration increases by 5 orders of magnitude.

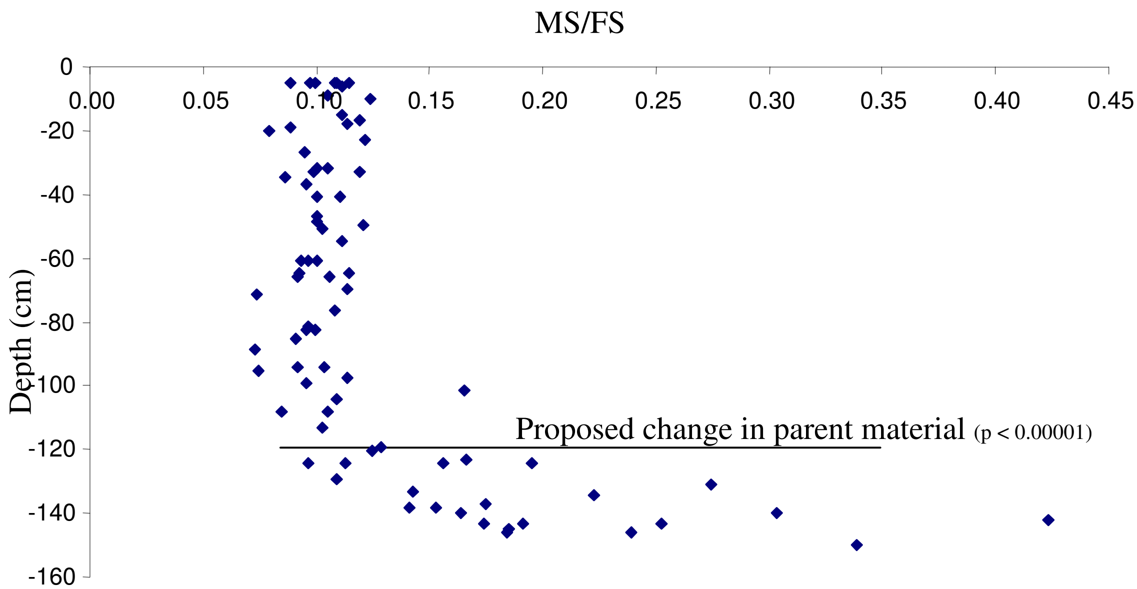

Fig. 4.7 Sand grain analysis of composited horizon samples across grid. Ratios are expressed in terms of percent medium sand (MS) to fine sand (FS) in the coarse fraction. Analysis of variance and t-tests were used for separate parent materials at 1.2 m, maximizing the difference between the mean sand size fractions.

Transect 8,0 – 8,40

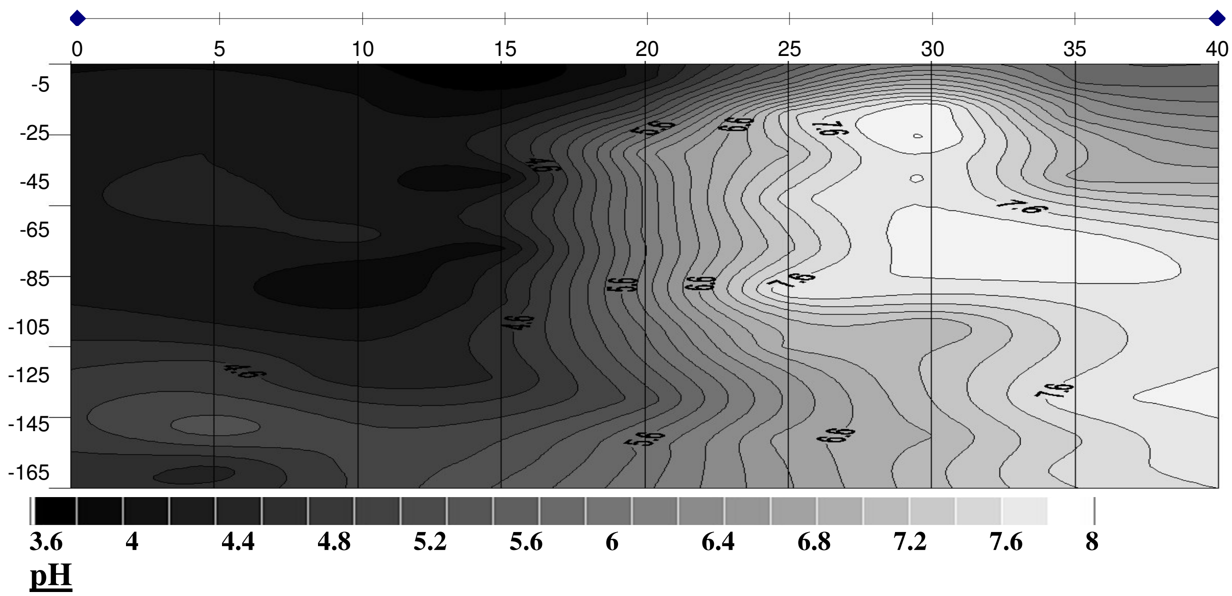

Fig. 4.8. Profile showing $pH_{2:1}$ for transect 8,0 – 8,40. The profile pH ranges from 3.5 to 8.2 within 15 m. Contours show 0.2 pH unit intervals.

The abruptness of the association could be explained by the buffering capacity of the spodic system, where high concentrations of chelated Al are found. Where the sodium-rich waters encroach, there appears to be a correlation with lower pH (Fig 4.9). This results from ion exchange, where Al is displaced from the strong organic complexes, and is free to hydrolyze water.

The alkaline pH in the argillic resulted from dissolution of oyster fragments. Shells were commonly found within the horizons but showed no orientation and were well mixed within the upper 25 cm. The cation exchange capacity was unusually high for this region. Deionized water extracts (2:1) were made and cation concentrations measured to determine the contribution of soluble cations in the soil solution.

The soluble cation concentrations were examined to compare the soil solution to that of seawater (Table 4.2) to determine whether saltwater influence contributes to the formation of subsurface horizons. In this case, there were high concentrations of Na at depth, and the ratios of Mg/Ca, Na/Mg, and Mg/K reflected those of seawater chemistry, indicating seawater contribution at depth (Fig 4.10). The figure shows appreciable amounts of dissolved Ca in 8,30, whereas 8,15 contained very little soluble Ca. This results from the high cation exchange capacitance in the organic rich horizons. The dominance of Na at depth is apparent from both profiles, where the maximum value in 8,15 occurs just above the water table.

CONCLUSIONS

The dramatic contrast between the two soil types gave indication that this soil association has many factors influencing the pedogenic development. The lateral

Transect 8,0 – 8,40

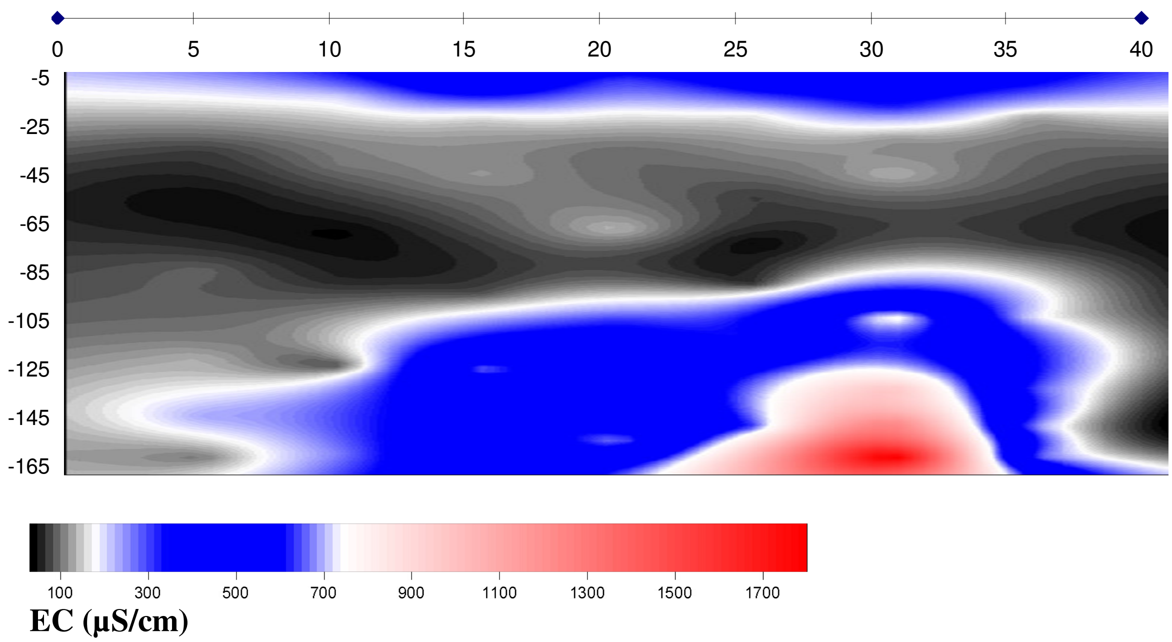

Fig. 4.9. Soil electrical conductivity measured from a 2:1 deionized water extract. The plot shows the wide range of EC at depth, and across the transect. The highest conductivity appears as a bulge occurring just below the maximum pH for this transect, corresponding to high Na concentration.

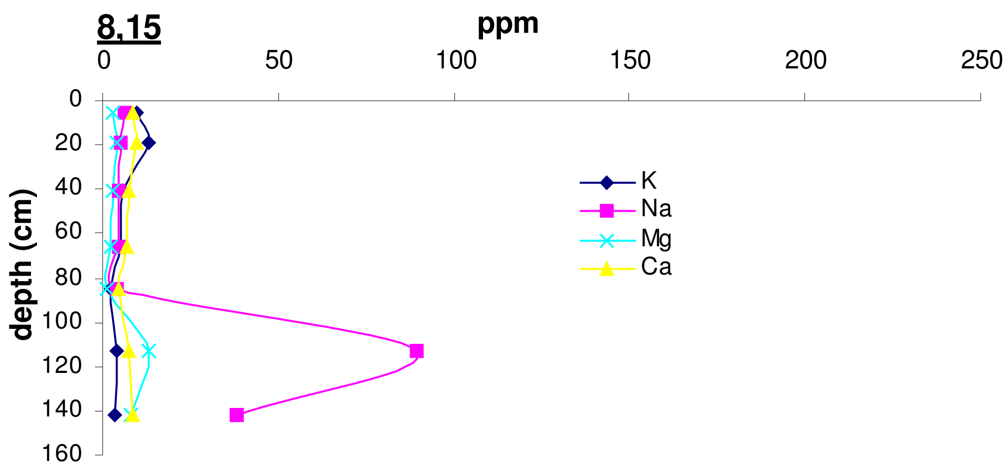

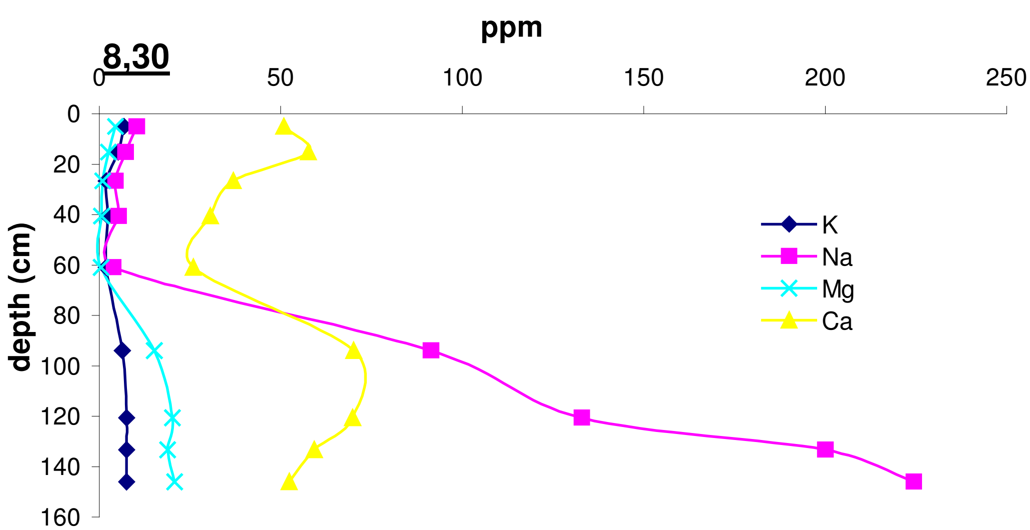

Fig 4.10. Profiles of dissolved cations at 8,15 and 8,30 in the soil solution (scaled to gravimetric moisture content at time of sampling).

Table 4.2. A comparison between typical sea water and soil solution chemistry found within two pedons.[1]

Major Cation Concentrations in Seawater[1]

Dissolved species		-------Cation ratios-----		
cation	ppm	Mg/Ca	Na/K	Mg/K
Na	11017	3.11	28.25	3.35
Mg	1308			
Ca	420			
K	390			

Soluble Cation Concentrations for Selected Soil Profiles

8,15

cm depth	K	Na	Ca	Mg	total	Mg/Ca	Na/K	Mg/K
	ppm							
5.08	9.79	6.41	8.44	2.71	45.93	0.32	0.65	0.28
19.05	13.02	5.16	9.89	3.93	53.83	0.40	0.40	0.30
40.64	5.62	4.83	7.52	2.67	37.15	0.36	0.86	0.48
66.04	4.93	4.81	6.71	2.37	33.86	0.35	0.98	0.48
85.09	2.55	4.20	4.65	1.29	22.94	0.28	1.65	0.50
113.03	3.95	89.25	7.64	13.07	212.68	1.71	22.59	3.31
142.24	3.29	37.88	8.46	7.95	109.85	0.94	11.50	2.41

8,30

cm depth	K	Na	Ca	Mg	total	Mg/Ca	Na/K	Mg/K
	ppm							
5.08	6.72	10.32	50.82	4.35	137.45	0.09	1.54	0.65
15.24	5.21	7.19	57.55	2.43	137.53	0.04	1.38	0.47
26.67	1.98	4.45	36.94	0.81	84.19	0.02	2.25	0.41
40.64	2.38	5.33	30.60	0.53	72.81	0.02	2.24	0.22
60.96	1.93	3.99	25.83	0.45	60.51	0.02	2.07	0.23
93.98	6.38	91.39	70.05	15.12	347.08	0.22	14.32	2.37
120.65	7.55	132.92	69.82	20.17	434.64	0.29	17.60	2.67
133.35	7.46	200.00	59.18	18.73	522.89	0.32	26.82	2.51
146.05	7.54	224.44	52.28	20.65	557.16	0.39	29.78	2.74

[1] From Langmuir, 1997

abruptness of the soil boundary suggests that the clay rich horizon resulted from deposition rather than illuvation. It is possible that the associated depression resulted from the dewatering and compaction of clay-rich sediments under the meter of material. Recent studies suggest that this mechanism is one of the driving forces behind barrier island migration (P. Gayes, Coastal Carolina, pers com.).

Regardless of the initial source of this association, it appears that two different processes are at work producing diverging profiles. Evidence suggested that E horizon morphology resulted from two contrasting processes, one where Fe is reduced and transported in solution, and the other where leseivage of organic rich solutions bleached the sands. Overlying the clay-rich horizon, the depth to the top of the E remained constant. There were also common occurrences of plinthite where the top of the E met the epipedon. This suggests that Fe was reduced during localized perching of the ground water and oxidized on top leading to the formation of this E horizon. Overlying the spodic layer, the top of the E paralleled the observed water table. This suggests that the E horizon may have formed from the migration of organic acids through the profile and deposited at depth.

The high ionic strength of the ground water suggests a mechanism where the complexed carbon/sesquioxide solution is precipitated due to flocculation. The highly charged organo-metallic substances travel through the profile, they repel each other. But, when the suspension encounters waters with high ionic strength, the activity of the solution is increased, effectively decreasing the solubility of the dissolved species.

As mentioned earlier, it appears that the two profiles are diverging from one another. The vegetation found in this environment changes abruptly and the plant species reflect this change. Many speculate that this change reinforces the soils developed in respect to this, as the nutrient cycling occurs from plant uptake at depth and deposition in the epipedon. The development of spodic horizons exemplifies this feedback mechanism. Pine and water oak species thrive in acid environments, where they deposit copious amounts of acid plant material. This, in turn, acidifies the soil beneath and allows organic substances to move through the profiles, unimpeded by microbial decay. In the base-rich material, grasses and palms thrive in the more neutral conditions. In turn, they deposit Ca-rich detritus to be cycled back into to the soil.

REFERENCES

Bui, E.N., J.M. Mazzullo, and L.P. Wilding. 1989. Using quartz grain size and shape analysis to distinguish between Aeolian and fluvial deposits in Dallal Bosso of Niger (West Africa). Earth Sys. Proc. and Landforms. 14: 157-166.

Ciolkosz, E.J., Waltman, W.J., Simpson, T.W., and Dobbs, R.R., 1989. Distribution and genesis of soils of the northeastern United States. Geomorphology 2: 285-302.

Davis, R.A. 1992. Depositional systems. An introduction to sedimentology and stratigraphy. Prentice Hall, New Jersey. 604 p.

Farmer, V.C., J.D. Russell, and M.L. Berrow. 1980. Imogolite and proto-imogolite allophane in spodic horizons: Evidence of a mobile aluminum silicate complex in poszol formation. J. Soil Sci. 31:673-684.

Gardner, L.R., B.R. Smith, W.K. Michener. 1992. Soil evolution along a forest-salt marsh transect under a regime of slowly rising sea level, southeastern United States. Geoderma 55:141-157.

Golden Software, Inc. 2000. Surfer 7. Golden Software, Inc., Golden Colorado.

Hoyt, J..H., and V.J. Henry Jr. 1967. Influence of island migration on barrier-island sedimentation. Geol. Soc. Am. Bull. 78:77-86.

Hoyt, J.H., and J.R. Hails. 1967. Pleistocene shoreline sediments in coastal Georgia; deposition and modification. Science 3769:1541-1543.

Langmuir, D.L. 1997. Aqueous Environmental Geochemistry. Prentice-Hall, Inc., New Jersey.

Markewich, H.W., M.J. Pavich, M.J. Mausbach, B.N. Stuckey, R.G Johnson, and V.M. Maryland Gonzalex. 1987. Age relations between soils and geology in the Coastal Plain of and Virginia. U.S. Geol. Sur. Bul. 1589A:34 pp.

Miller, W.P. and D.M. Miller. 1987. A micro-pipette method for soil mechanical analysis. Comm. in Soil Sci. Plant Anal. 18(1).

Oertel, G.F. 1979. Barrier island development during the Holocene recession, Southeastern United States. *In* Leatherman, S.P. (ed.) Barrier islands: from the Gulf of St. Lawrence to the Gulf of Mexico. Academic Press, Inc. New York.

Phillips, J.D. 2001. Contingency and generalization in pedology, as exemplified by texture-contrast soils. Geoderma 102:347-370.

Phillips, J.D., D. Perry, A.R. Garbee, K. Carey, D. Stein, M.B. Morde, J.A. Sheehy. 1996. Deterministic uncertainty and complex pedogenesis in some Pleistocene dune soils. Geoderma 73:147-164.

Rhoades, J.D. 1996. Salinity: Electrical conductivity and total dissolved solids. p. 417-435. *In* D.L. Sparks et al. (ed.) Methods of soil analysis. Part 3. Chemical methods. SSSA Book Ser. 5. SSSA and ASA, Madison, WI.

Shaw, J.N., and M.C. Rabenhorst. 1999. Pedogenic and morpholocial characteristics of marl-derive soils in the Ridge and Valley Province, Eastern United States. Soil Sci. 164 (12): 936-945.

Sumner, M.E. and W.P. Miller. 1996. Cation exchange capacity and exchange coefficients. p. 1201-1229. *In* D.L. Sparks et al. (ed.) Methods of soil analysis. Part 3. Chemical methods. SSSA Book Ser. 5. SSSA and ASA, Madison, WI.

Tan, Z., W.G. Harris, and R.S. Mansell. 1999. Water table dynamics across and aquod-udult transition in Florida flatwoods. Soil Sci. 164:10-17.

CHAPTER 5

SUMMARY AND CONCLUSIONS

I undertook this study in an effort to unveil some of the processes involved in barrier island formation. Like most projects, what we expected to see is not what we found. What we did find, however, was a perfect opportunity to test the use of GPR in application to soil sciences. With the help of geochemical analysis, a little light has been shed on the dark subject of spodosols.

Like most of the Coastal Plain Region of the Southeast, Skidaway Island has soil associations which contain dramatic texture contrasts. The lateral heterogeneity associated with the aquod/udult association provided an ideal environment to examine new methodologies for pedological investigation. Ground penetrating radar worked well to map the boundary in this environment. The increase in clay dramatically attenuated the GPR signal, enabling us to see the soil boundary in the field while profiling. The difference was accentuated by setting the gain parameters to maximize signal recovery in the less conductive media. Although the individual profiles showed this change, slicing the data clearly improved the interpretability of the profiles. The partially-indurated ortstein layer produced point-source reflections, which were visible on profile maps and used to calculate the electromagnetic wave velocity for accurate determination of depth to reflecting media.

This type of environment was ideal for GPR, representing a "best case" scenario, due to dramatic changes in dielectric properties of the soil horizons. It should be noted that this case only exists in depositional environments or where pedogenic development has produced abrupt changes in the soil dielectric. The use of GPR is limited to these types of environments based on the fundamental properties of electromagnetic reflection, which are a function of the change in dielectric and the distance that the change occurs over.

The dramatic contrast between the two soil types gave indication that this soil association has many factors influencing the pedogenic development. The lateral abruptness of the soil boundary suggests that the clay rich horizon resulted from deposition rather than illuvation. It is possible that the associated depression resulted from the dewatering and compaction of clay-rich sediments under the meter of material, as has recently been suggested as a mechanism for barrier island migration.

The morphology of the adjacent E horizon appeared to result from two uniquely differing processes. One can be explained by upward migration of Fe resulting from the reduction and subsequent dissolution and transport. In the spodic, it appeared that lessievage of organic acids generated the spodic and E horizons. Where salt water influenced the ground water chemistry, flocculation of the Al/COOH complex may occur, which is suggested as the mechanism for spodosol genesis on Skidaway Island.

It appears that the two contrasting profiles resulted from marine conditions, rather than those associated with terrestrial conditions. It is assumed that they are diverging from one another, due to the dramatic shift in vegetation. Many speculate that this change reinforces the soils developed in respect to this, as the nutrient cycling occurs from plant uptake at depth and deposition in the epipedon. The development of spodic horizons exemplifies this feedback mechanism, where pine and water oaks deposit acid-rich organic debris. The argillic horizon provides copious amounts of exchangeable Ca, allowing grasses and palms to thrive in the region. In turn, they deposit Ca-rich detritus to be cycled back into to the soil, completing the cycle.

REFERENCES

Aiken, G.R., D., M. McKnight, and R.L. Wershaw. 1985. Humic substances in soil, sediments, and water. Wiley (Interscience), New York.

Annan, A.P., and S.W. Cosway. 1992. Ground-penetrating radar survey design: Proc. of the Symp. on the Application of Geophysics to Eng. and Environ. Problems (SAGEEP).

Bergelin, A., P.A.W. van Hees, O. Wahlberg, and U.S. Lundström. 2000. The acid-base properties of high and low molecular weight organic acids in soil solutions of podzolic soils. Geoderma 94:223-235.

Boll, J., R.P.G. van Rijn, K.W. Weiler, J.A. Ewen, J. Daliparthy, S.F. Herbert, and T.S. Steenhuis. 1996. Using ground-penetrating radar to detect layers in a sandy field soil. Geoderma 70:117-132.

Bui, E.N., J.M. Mazzullo, and L.P. Wilding. 1989. Using quartz grain size and shape analysis to distinguish between Aeolian and fluvial deposits in Dallal Bosso of Niger (West Africa). Earth Sys. Proc. And Landforms. 14: 157-166.

Buol, S.W, F.D. Hole, R.J. McCracken, and R.J. Southard. 1997. Soil genesis and classification. Iowa Sate University Press, Ames, Iowa.

Burgess, A. and D.P. Drover. 1953. The rate of podzol development in sands of the Woy district N.S.W. Aus. J. Bot. 1:83-94.

Chan, C., and R. Knight. 2001. Laboratory measurements of electromagnetic wave velocity in layered sands. Water Resour. Res. 37:1099-1105.

Chesworth, W. 1973. The parent rock effect in the genesis of soil. Geoderma 10:215-225.

Ciolkosz, E.J., Waltman, W.J., Simpson, T.W., and Dobbs, R.R., 1989. Distribution and genesis of soils of the northeastern United States. Geomorphology 2: 285-302.

Collins, M.E., and J.A. Doolittle. 1987. Using ground-penetrating radar to study soil microvariability. Soil Sci. Soc. Am. J. 51:491-493.

Conyers, L. and D. Goodman. 1997. Ground-penetrating radar-An introduction for archaeologists. Altamira Press, Walnut Creek, California.

Daniels, Davis, R.A. 1992. Depositional systems. An introduction to sedimentology and stratigraphy. Prentice Hall, New Jersey. 604 p.

Daniels, D.J. 1996. Surface-penetrating radar-IEE radar, sonar, navigation and avionics Series 6: London, The Institute of Electrical Engineers.

Davis, J.L. and Annan, A.P. 1989. Ground-penetrating radar for high-resolution mapping of soil and rock stratigraphy. Geophysical Prospecting 37:531-551.

DeConnick, F. 1980. Major mechanisms in formation of spodic horizons. Geoderma 24:101-123.

Doolittle, J.A. 1982. Characterizing soil map units with the ground-penetrating radar. Soil Surv. Hor. 23(4):3-10.

Doolittle, J.A. 1987. Using ground-penetrating radar to increase quality and efficiency of soil surveys. p. 11-32 *In* W.U. Reybold and G.W. Petersen (ed.) Soil survey techniques. SSSA Spec. Publ. 20. SSSA, Madison, WI

Farmer, V.C., J.D. Russell, and M.L. Berrow. 1980. Imogolite and proto-imogolite allophane in spodic horizons: Evidence of a mobile aluminum silicate complex in podzol formation. J. Soil Sci. 31:673-684.

Gardner, L.R., B.R. Smith, W.K. Michener. 1992. Soil evolution along a forest-salt marsh transect under a regime of slowly rising sea level, southeastern United States. Geoderma 55:141-157.

Geisler, R., H. Ilvesniemi, L. Nyberg, P. van Hees, M. Starr, K. Bishop, T. Kareinen, U.S. Lundström. 2000. Distribution and mobilization of Al, Fe, and Si in three podzolic soil profiles in relation to the humus layer. Geoderma 2000:249-263.

Greaves, R.J., D.P. Lesmes, J.M. Lee, and M.N. Toksöz. 1996. Velocity variations and water content estimated from multi-offset, ground-penetrating radar. Geophys. 61:683-695.

Geophysical Survey Systems Incorporated. 2001. RADAN for Windows NT. Geophysical Survey Systems, Inc. North Salem, New Hampshire.

Golden Software, Inc. 2000. Surfer 7. Golden Software, Inc., Golden Colorado.

Harris, W.G, and K.A. Hollien. 1999. Changes in quantity and composition of crystalline clay across E-Bh boundaries of Alaquods. Soil Sci. 164:602-608.

Harris, W.G., and K.A. Hollien. 2000. Changes across artificial E-Bh boundaries formed under simulated fluctuating water tables. Soil Sci. Soc. Am. J. 64:967-973.

Hayes, M.O. 1994. The Georgia Bight barrier system. *In* Davis, R.A. (ed.) Barrier islands. Springer-Verlag, New York. pp.233-304

Hoyt, J.H., and V.J. Henry Jr. 1965. Significance of inlet sedimentation in the recognition of ancient barrier islands. *In.* Pleistocene and Holocene sediments, Sapelo Island, Ga., and vicinity. Geol. Soc. Am. SE Sec. Field Trip 1, 1966, Guidebook.

Hoyt, J.H., and V.J. Henry Jr. 1967. Influence of island migration on barrier-island sedimentation. Geol. Soc. Am. Bull. 78:77-86.

Hoyt, J.H., and J.R. Hails. 1967. Pleistocene shoreline sediments in coastal Georgia; deposition and modification. Science 3769:1541-1543.

Jackson, P.D., D.T. Smith, and P.N. Stanford. 1978. Resistivity-porosity-particle shape relationships for marine sands. Geophysics 43:1250-1268.

Jenny, H. 1941. Factors of Soil Formation. McGraw-Hill, New York.

Johnson, M.G., and M.B. McBride. 1989. Mineralogical and chemical characteristics of Adirondack Spodosols: Evidence for para- and noncrystalline alluminosilicate minerals. Soil Sci. Soc. Am. J. 53:483-490.

Johnson, R.W., R. Glaccurn, and R. Wojtansinski. 1980. Application of ground-penetrating radar to soil survey. Proc. Soil Crop Sci. Soc. Fla. 39:68-72.

Langmuir, D.L. 1997. Aqueous Environmental Geochemistry. Prentice-Hall, Inc., New Jersey.

Lee, F.Y., T.L. Yuan, and V.W. Carlisle. 1988. Nature of cementing materials in orstein horizons of selected Florida Spodosols: II. Soil properties and chemical form(s) of aluminum. Soil Sci. Soc. Am. J. 52:1796-1801.

Lundström, U.S., N. van Breemen, and D. Bain. 2000a. The podzolization process. A review. Geoderma 94:91-107.

Lundström, U.S., N. van Breemen, D.C. Bain, P.A.W. van Hees, R. Geisler, J.P. Gustafsom, H. Ilvesniemi, E. Karltun, P. –A. Melkerud, M. Olsson, G. Riise, O. Wahlberg, A. Bergelin, K. Bishop, R. Finlay, A.G. Jongmans, T. Magmisson, H. Mamerkoski, A. Nordgren, L. Nyberg, M. Starr, L. Tau Strand. 2000b. Advances in understanding the podzolization process resulting from a multidisciplinary study of three coniferous forest soils in the Nordic Countries. Geoderma 94: 335-353.

MacNeil, F. 1950. Pleistocene shorelines in Florida and Georgia. Shorter contributions to general geology, 1949. Geol. Sur. Prof. Paper 221-F. p. 95-107.

Markewich, H.W., M.J. Pavich, M.J. Mausbach, B.N. Stuckey, R.G Johnson, and V.M. Maryland Gonzalex. 1987. Age relations between soils and geology in the Coastal Plain of and Virginia. U.S. Geol. Sur. Bul. 1589A:34 pp.

Markewich H.W., and M.J. Pavich. 1991. Soil chronosequence studies in temperate to subtropical, low-latitude, low-relief terrain with data from the eastern United States. Geoderma 51:213-239.

McKeague, J.A. 1968. Humic-fulvic acid ratio, Al, Fe, and C in pyrophosphate extracts as a criteria of A and B horizons. Can. J. Soil Sci. 48:27-35

McKeague, J.A, F. DeConnick, and D.P. Franzmeir. 1982. Spodosols p. 216-248. *In* Wilding L.P.(ed.), Pedogenesis and Soil Taxonomy. II. Elsevier, Developments in Soil Science 11B.

Melkerud, P.-A., D.C. Bain, A.G. Jongmans, and T. Tarvainen. 2000. Chemical, mineralogical and morphological characterization of three podzols developed on glacial deposits in Northern Europe. Geoderma 94:125-148.

Miller, W.P. and D.M. Miller. 1987. A micro-pipette method for soil mechanical analysis. Comm. in Soil Sci. Plant Anal. 18(1).

Mokma, D.L. and P. Buurman. 1982. Podzols and podzolization in temperate regions. ISSM monograph 1, Int. Soil Museum, Wageningen, 126 pp.

Mokma, D.L, R.J. Schaetzl, J.A. Doolittle, and E.P. Johnson. 1990. Ground-penetrating radar study of orstein continuity in some Michigan Haplaquods. Soil Sci. Soc. of Am. J. 54:936-938.

Oertel, G.F. 1979. Barrier island development during the Holocene recession, Southeastern United States. *In* Leatherman, S.P. (ed.) Barrier islands: from the Gulf of St. Lawrence to the Gulf of Mexico. Academic Press, Inc. New York.

Olson, C.G. and J.A. Doolittle. 1985. Geophysical techniques for reconnaissance investigations of soils and surficial deposits in mountainous terrain. Soil Sci. Soc. Am. J. 49:1490-1498.

Phillips, J.D. 2001. Contingency and generalization in pedology, as exemplified by texture-contrast soils. Geoderma. 102:347-370.

Phillips, J.D., D. Perry, A.R. Garbee, K. Carey, D. Stein, M.B. Morde, J.A. Sheehy. 1996. Deterministic uncertainty and complex pedogenesis in some Pleistocene dune soils. Geoderma 73:147-164.

Phillips, L.P., N.B. Comerford, D.G. Neary, and R.S. Mansell. 1999. Simulation of soil water above a water table in forested Spodosol. Soil Sci. Soc. Am. J. 53:1236-1241.

Reppert, P.M., F.D. Morgan, and M.N. Toksöz. 2000. Dielectric constant determination using ground-penetrating radar reflection coefficients. J. App. Geophys. 43:189-197.

Shaw, J.N., and M.C. Rabenhorst. 1999. Pedogenic and morpholocial characteristics of marl-derive soils in the Ridge and Valley Province, Eastern United States. Soil Sci. 164 (12): 936-945.

Skyllberg, Ulf and Ole Borggaard. 1998. Proton surface charge determination in Spodosol horizons with organically bound aluminum. Geochim et Cosmochim. Acta. 62:1677-1689.

Soil Survey Staff. 1960. Soil classification, a comprehensive system, 7th approximation. U.S. Government. Prtg. Off., Washington, D.C. 265 pp.

Soil Survey Staff. 1975. Soil Taxonomy: A basic system of soil classification for making and interpreting soil surveys. USDA-SCS Agric. Handb. 436. U.S. Gov. Print. Office, Washington, DC.

Sparks, D.R. 1995. Environmental Soil Chemistry. Academic Press, Inc. San Diego, California.

Stützer, A. 1998. Early stages of podzolisation in young aeolian sediments, western Jutland. Catena 32:115-129.

Tamm, O. 1950. Factors, which, in North Sweden, cause variations in the course of podsolization. Profile variants. *In* Buurman, P. (ed.) Podzols. Van Nostrand Reinhold Company Inc. 1984, pp. 174-198.

Tan, Z., W.G. Harris, and R.S. Mansell. 1999. Water table dynamics across and aquod-udult transition in Florida flatwoods. Soil Sci. 164:10-17.

U.S. Department of Agriculture – Soil Conservation Service. 1974. Soil survey of Bryan and Chathem Counties, Georgia. U.S. Government Printing Office, Washington, D.C.

Ugolini, F.C., and R.A. Dahlgren. 1991. Weathering environments and occurance of imogolite/allophane in selected andisols and Spodosols. Soil Sci. Soc. Am. J. 55:1116-1171.

Van Breemen, N., U.S. Lundström, and A.G. Jongmans. 2000. Do plants drive podzolization via rock-eating mycorrihizal fungi? Geoderma 94:163-171.

van Hees, P.A.W, U.S. Lundström, and R. Giesler. 2000. Low molecular weight organic acids and their Al-complexes in soil solution – composition, distribution and seasonal variation in three podzolized soils. Geoderma 94:173-200.

Wilson, P. 2001. Rate and nature of podzolisation in aeolian sands in the Falkland Islands, South Atlantic. Geoderma 101:77-86.

APPENDIX A

GENERAL SITE DESCRIPTION

A 40- by 15- m study grid was created encompassing a soil boundary where a Talquin fine sand (Arenic Alaquod) sharply grades to an Ocilla loamy sand (Arenic Umbric Paleaquult). The entire portion of the island is mapped as Leon fine sand and an Ellabelle loamy sand, which is completely misleading. Multiple trips around the island rarely produced spodic horizons. The site is located in Skidaway Island Sate Park, on the western-most side of the island. The site was chosen because of the spodosol-ultisol association and control over previous land managment.

The boundary between the soils is loosely reflected with a change in vegetation. The Talquin is dominated by loblolly pines (*Pinus tieda*) along with live and water oaks (*Quercus virginiana, Quercus nigra),* These trees are commonly draped in resurrection fern (*polypoduim polypodioides),* red bay (*Persea borbonia*) and yaupon holly (*Ilex vomitoria*) with very little understory. The finer textured Ocilla contains mostly cabbage palm (*Sabal palmetto)* and saw-palmetto (*Serenoa repens*) with thick, long-leaf grasses beneath.

Unlike most spodosols, there was not an appreciable O horizon in the majority of the area. Mostly, comprised of partially decomposed pine needles, it rarely accumulated more than 1-2" of organic debris in flat areas. Considerable piles of bark and pine needles commonly skirted the larger pines in the areas, occasionally exceeding 30cm thickness. In these areas, the mineral soil was well mixed, making it hard to distinguish the bottom of the O with the top of the A. The Ocilla soils appeared to have significantly less organic material on top. Much of the topsoil has signs of biological disturbances in the form of mole burrows; wild bore rooting; and very large ant mounds. Commonly, there were irreversibly hardened clay balls (1 cm) mixed in with the upper 10 cm or so. There were animal paths throughout the island usually leading to freshwater sloughs and small depressions found throughout the finer textured soils.

APPENDIX B

SOIL PROFILE DESCRIPTIONS

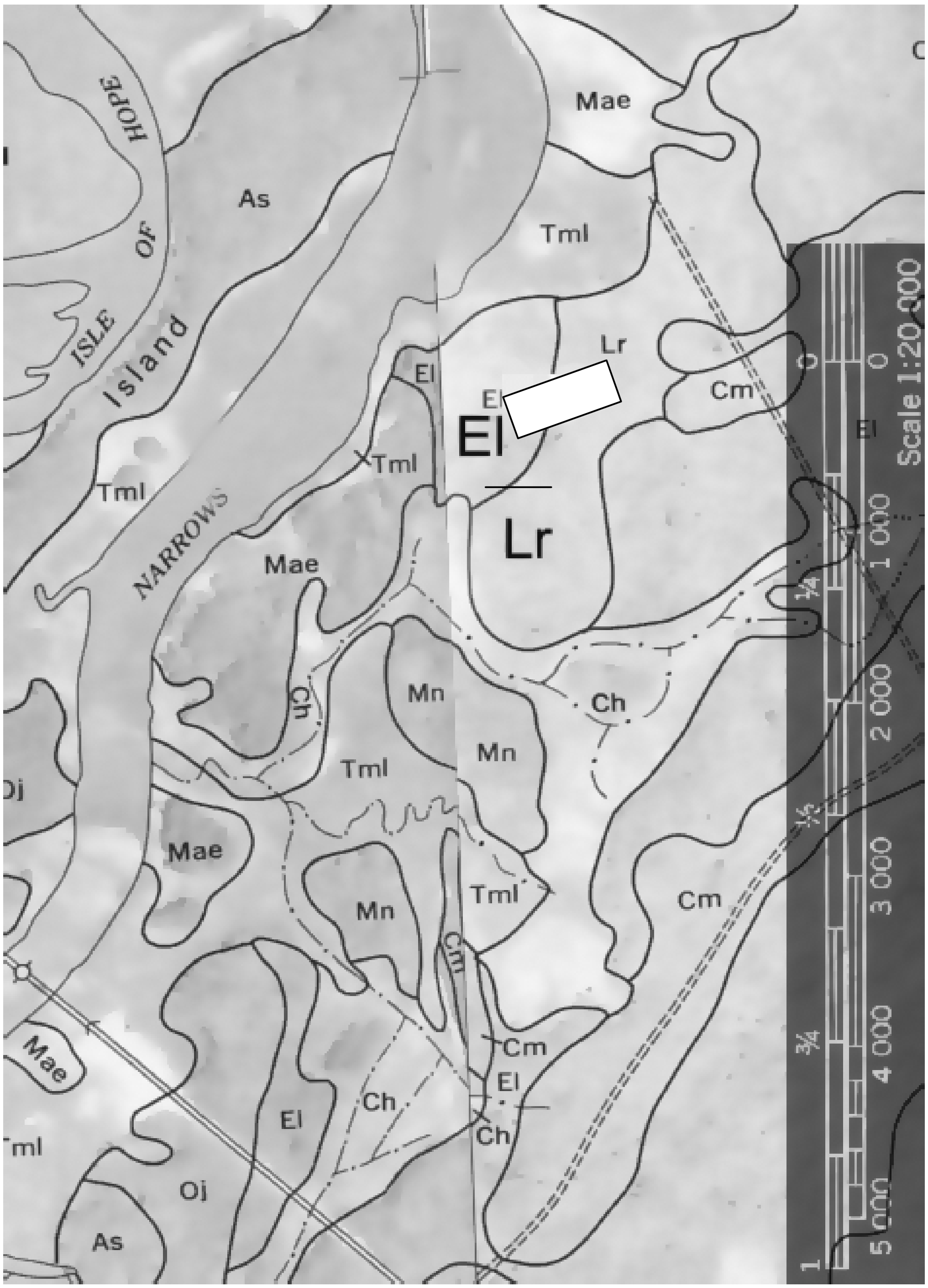

Location:

V02 -Skidaway Island State Park – heading towards the southern tip of the island (near Pioneer site #1)

(N 31’57’18.4”, W 081’03’23.1”)

Date Described:

Feb. 19, 2002

A 0-8” – black (2.5Y 2.5/1) fine sand; “salt-n-pepper” appearance; weak, medium, granular structure; “fluffy”; clear boundary.

AE 8-15” – dk. yellowish brown (10YR 4/4) fine sand; weak granular structure; very friable; abrupt boundary (sample: “S-V02-01”).

E 15-28” – light brownish gray (10YR 6/2) fine sand; many brown (7.5YR 2.5/3) friable nodules/inclusions; abrupt boundary

E/B 28-44” - very pale brown (10YR 7/4) fine sand with coarse strong brown (7.5YR 5/8) sandy clay loam inclusions/nodules; clear-abrupt boundary

C1 44-64” - pale brown (10YR 6/3) med-fine sand; massive; few firm prominent red nodules; abrupt boundary (samples: “S-VO2-03”)

possible artifact: 1” piece of angular plagioclase (sample: “S-VO2-03A) - see notebook for sketch.

C2 64-72”+ - light gray (N7) coarse-med sand, many coarse fragments; very wet; micaceous (sample: “S-VO2-04”)

V03 - Skidaway Island State Park – heading towards the southern tip of the island (near Pioneer site #1)

(N 31'57'18.3", W 081'03'23.5")

<u>Date described:</u>

Feb. 19, 2002

A 0-6” – very dark brown (10YR 2/2) fine sand; weak, granular structure; very friable; “salt-n-pepper”; fluffy; abrupt boundary

EB 6-26” – dark yellowish brown fine sand; weak subangular blocky structure; abrupt boundary

Bh 26-60” - brown (10YR 4/3) fine sand; massive

C 60-72” – med-coarse sand, many coarse organic matter nodules at bottom or horizon

APPENDIX C

EXCHANGEABLE CATION CONCENTRATIONS

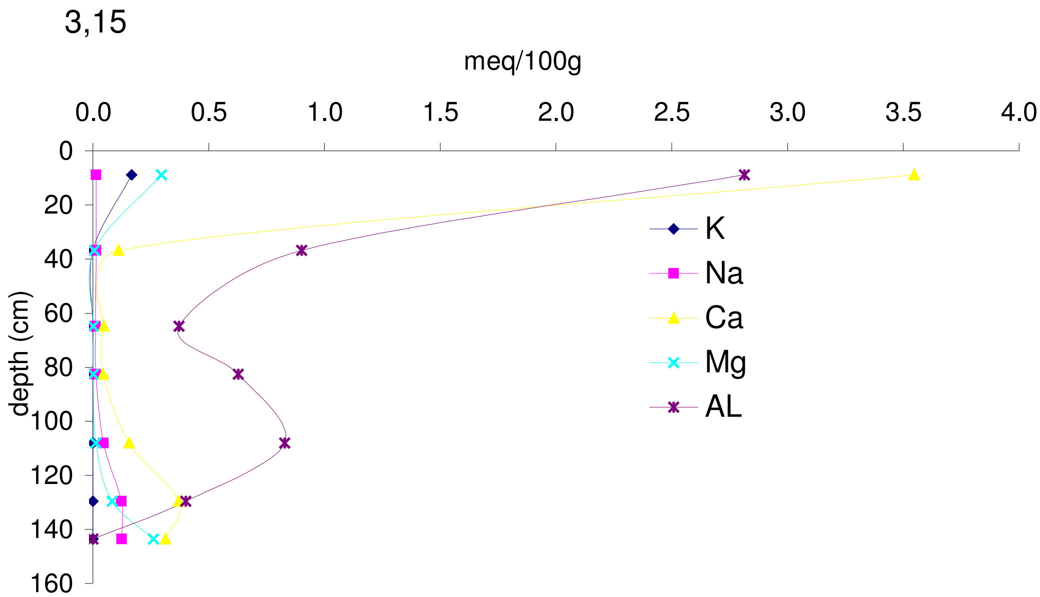

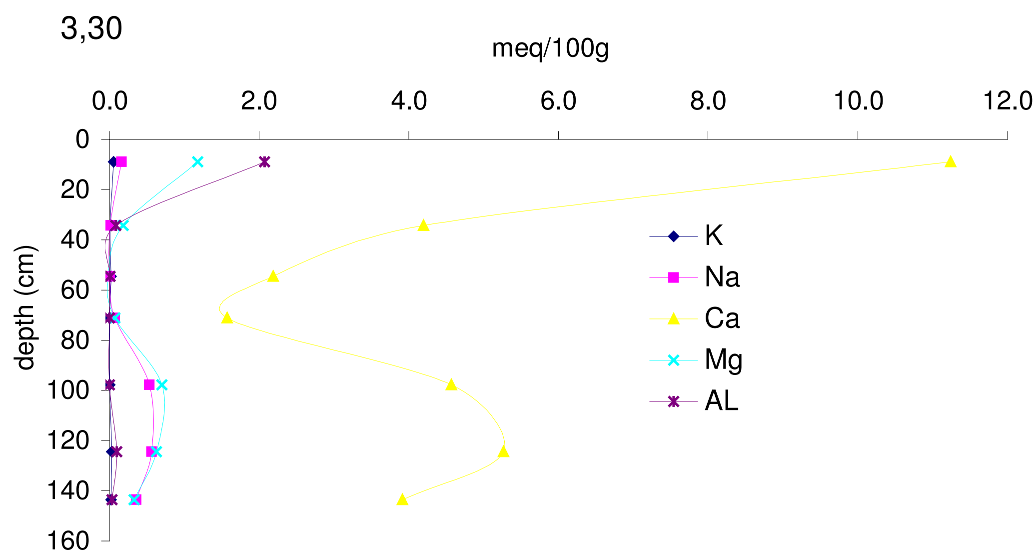

8,15

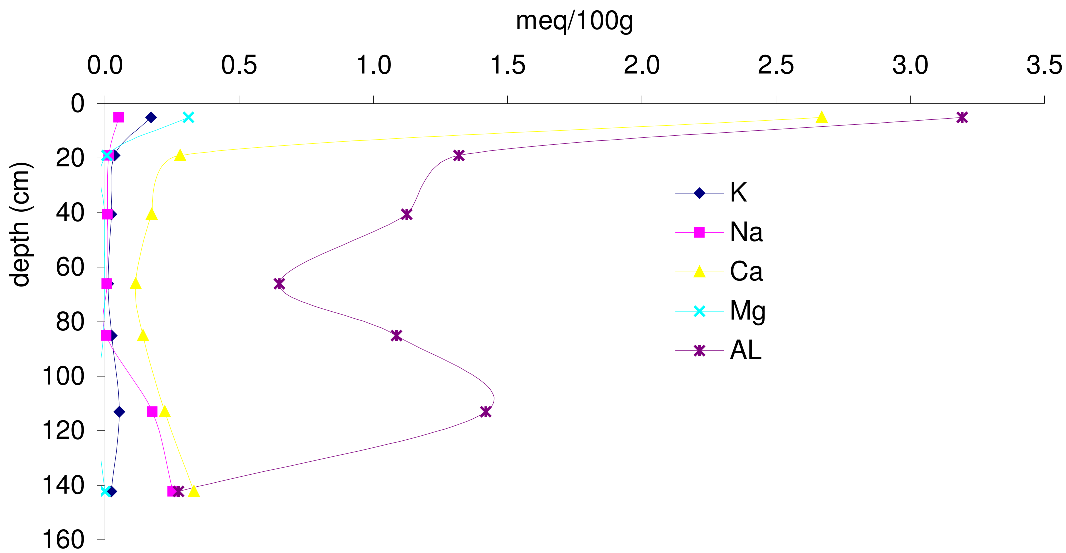
meq/100g
0.0
0.5
1.0
1.5
2.0
2.5
3.0
3.5
0
20
40
60
80
100
120
140
160
depth (cm)
K
Na
Ca
Mg
AL

8,30

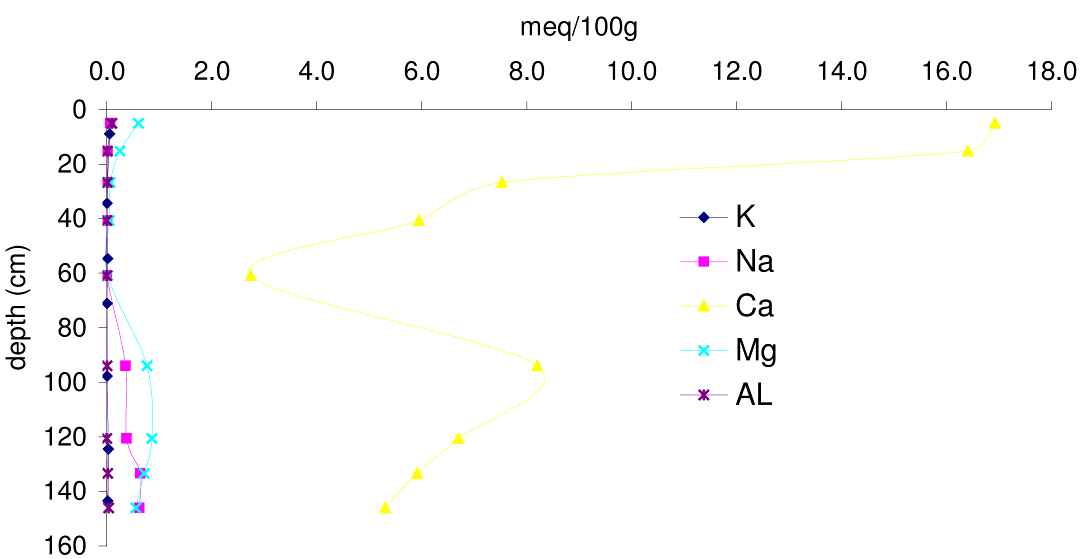
meq/100g
0.0
2.0
4.0
6.0
8.0
10.0
12.0
14.0
16.0
18.0
0
20
40
60
80
100
120
140
160
depth (cm)
K
Na
Ca
Mg
AL

13,15

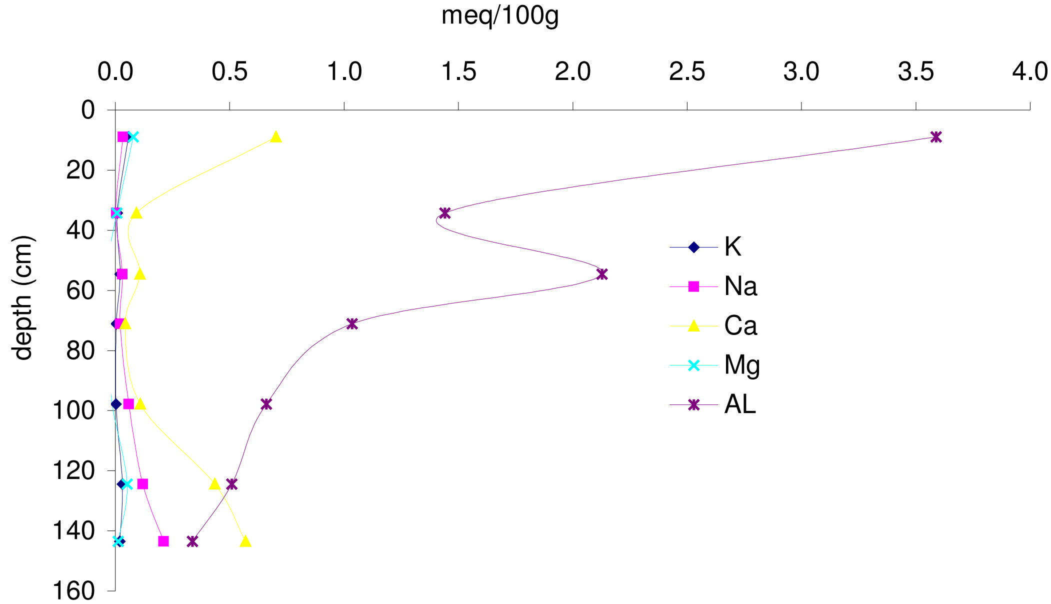
meq/100g
0.0
0.5
1.0
1.5
2.0
2.5
3.0
3.5
4.0
depth (cm)
0
20
40
60
80
100
120
140
160
K
Na
Ca
Mg
AL

13,30

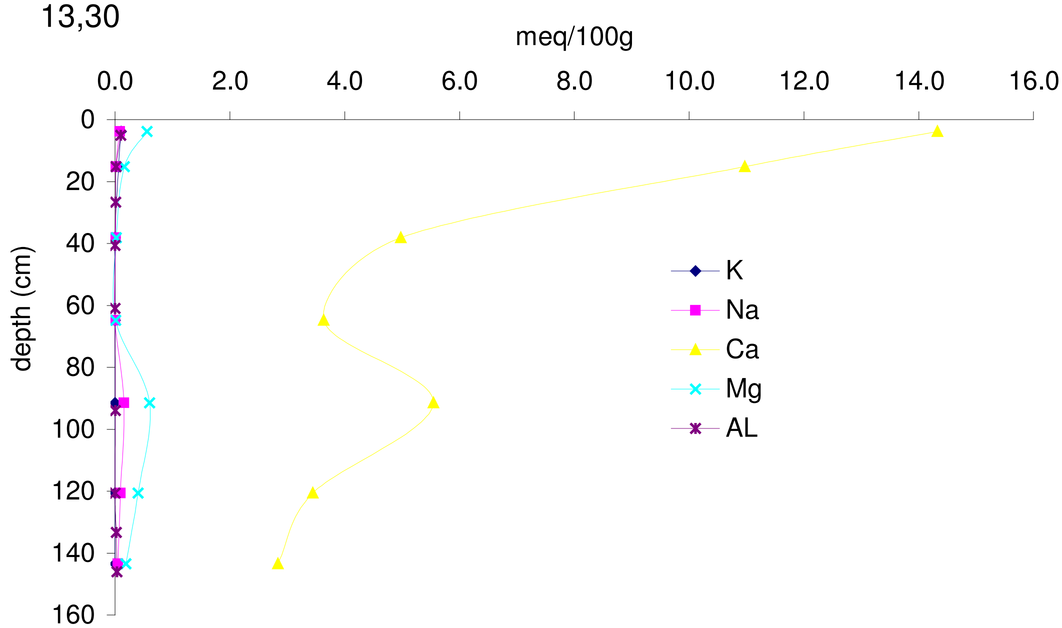
meq/100g
0.0
2.0
4.0
6.0
8.0
10.0
12.0
14.0
16.0
depth (cm)
0
20
40
60
80
100
120
140
160
K
Na
Ca
Mg
AL

APPENDIX D

BASIC CATIONS FROM DIONIZED WATER EXTRACTION

3,15

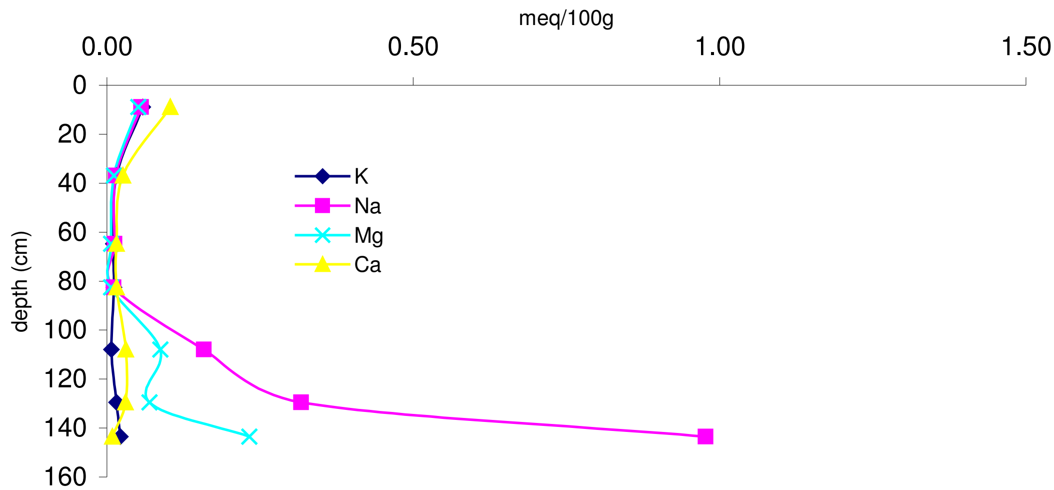

3,30

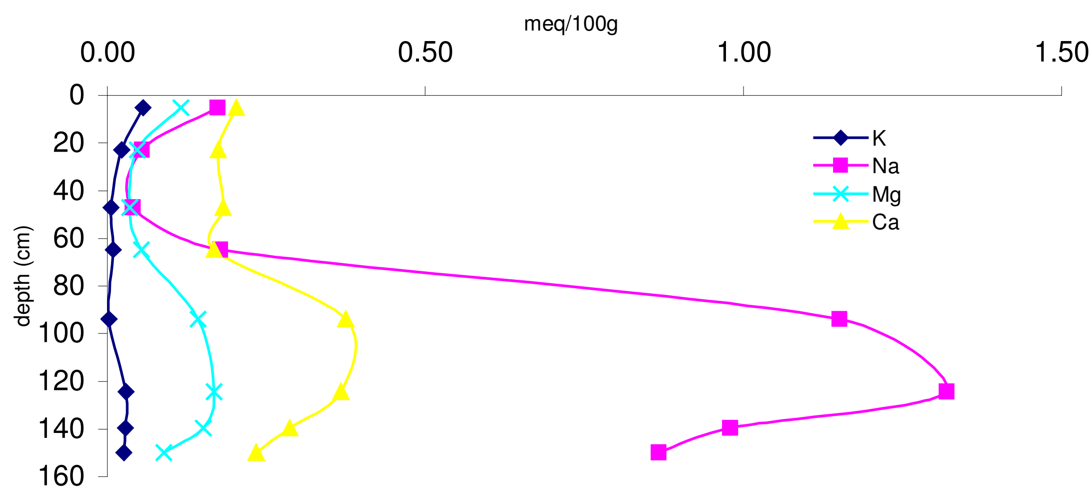

8,15

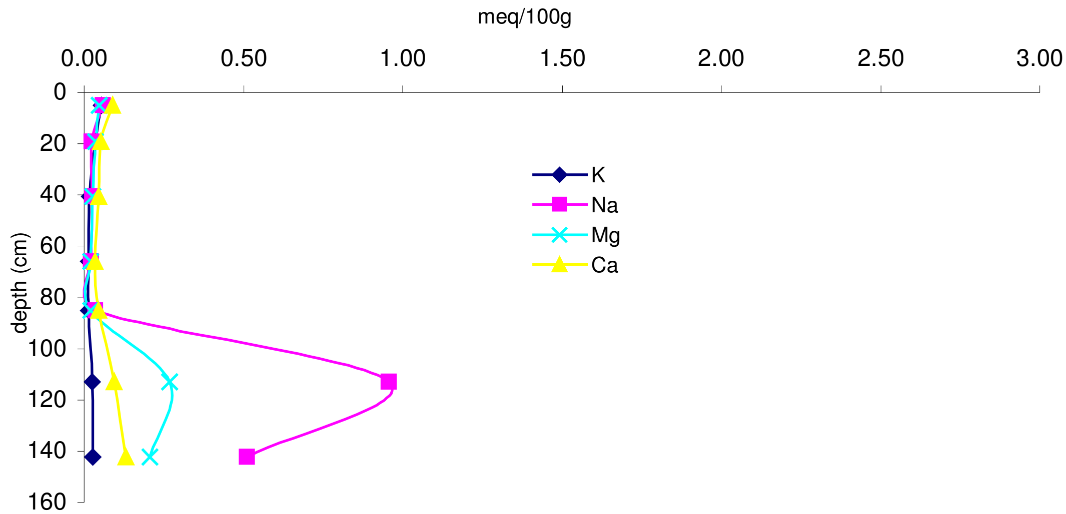
meq/100g
0.00
0.50
1.00
1.50
2.00
2.50
3.00
0
20
40
60
80
100
120
140
160
depth (cm)
K
Na
Mg
Ca

8,30

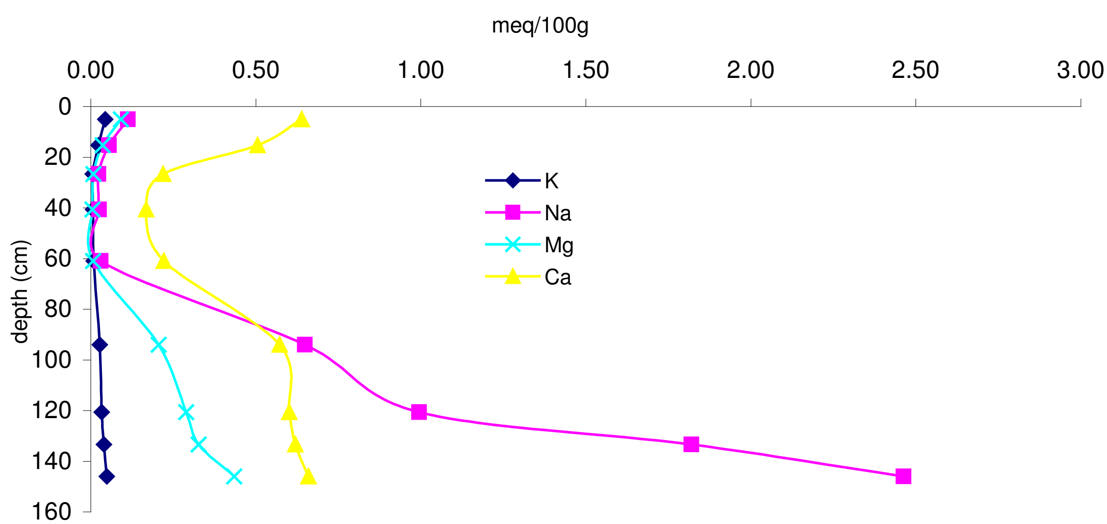
meq/100g
0.00
0.50
1.00
1.50
2.00
2.50
3.00
0
20
40
60
80
100
120
140
160
depth (cm)
K
Na
Mg
Ca

13,15

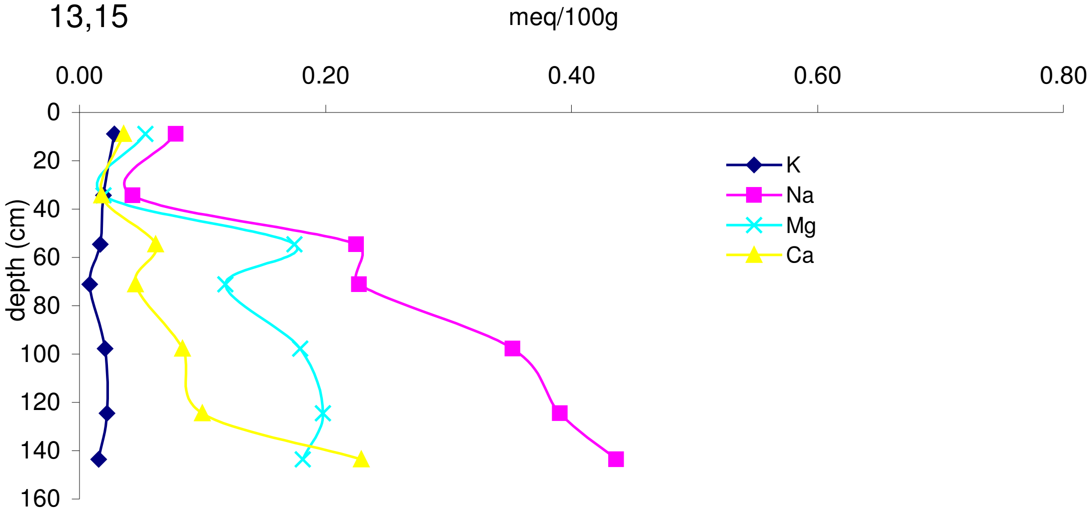
meq/100g
0.00
0.20
0.40
0.60
0.80
0
20
40
60
80
100
120
140
160
depth (cm)
K
Na
Mg
Ca

13,30

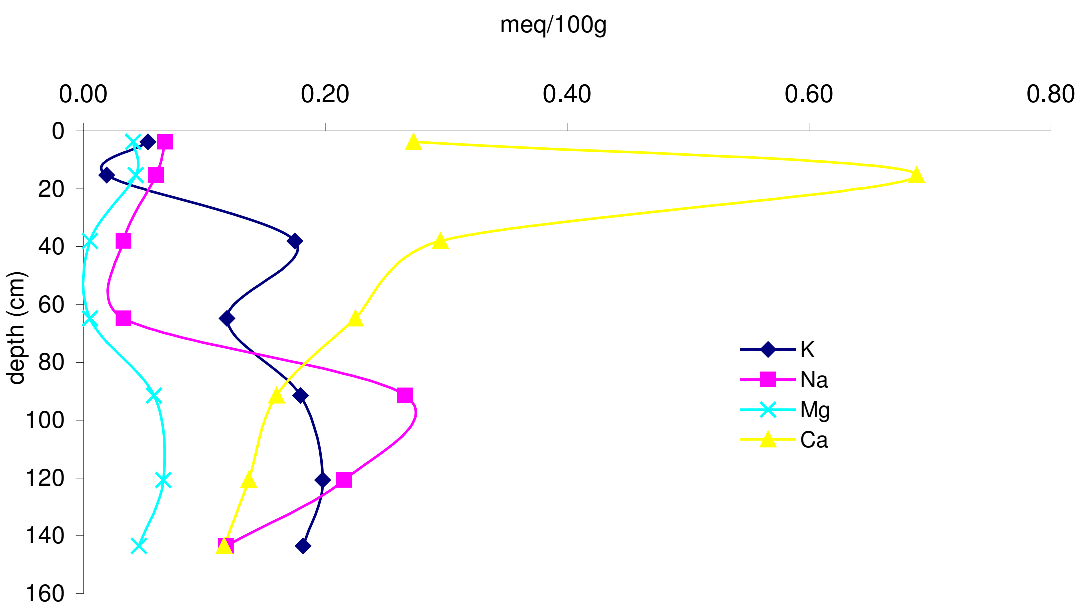
meq/100g
0.00
0.20
0.40
0.60
0.80
0
20
40
60
80
100
120
140
160
depth (cm)
K
Na
Mg
Ca

APPENDIX E

MOISTURE, ELECTRICAL CONDUCTIVITY AND pH PROFILES

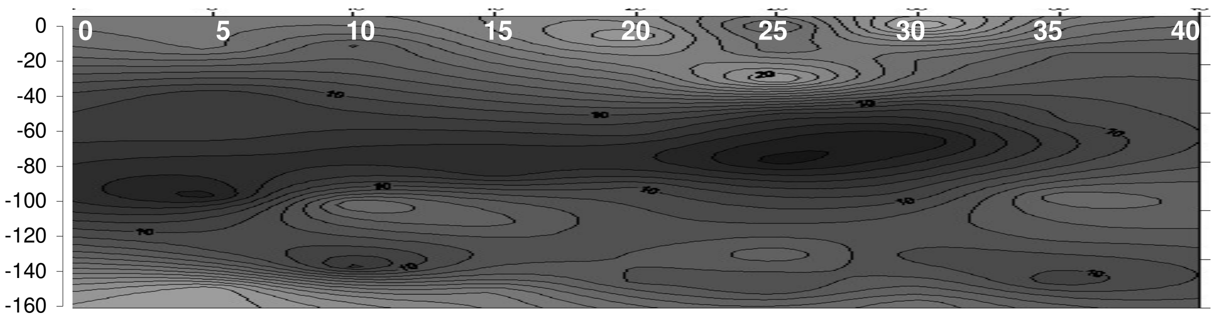

3,0 – 3,40

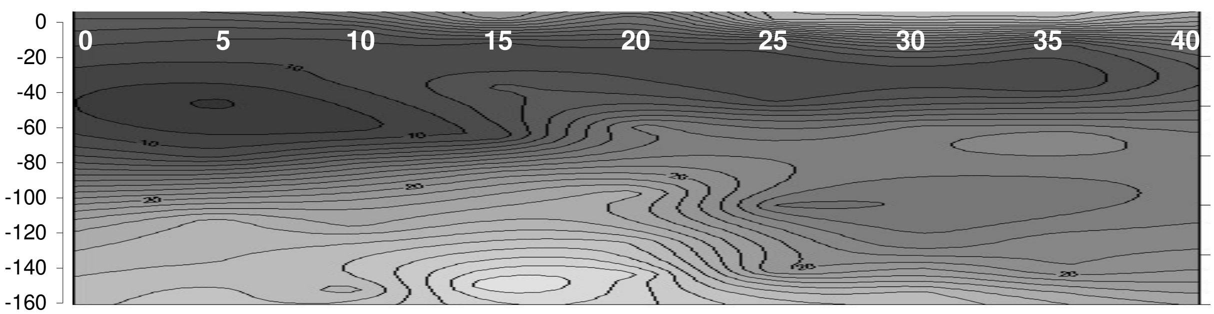

8,0 – 8,40

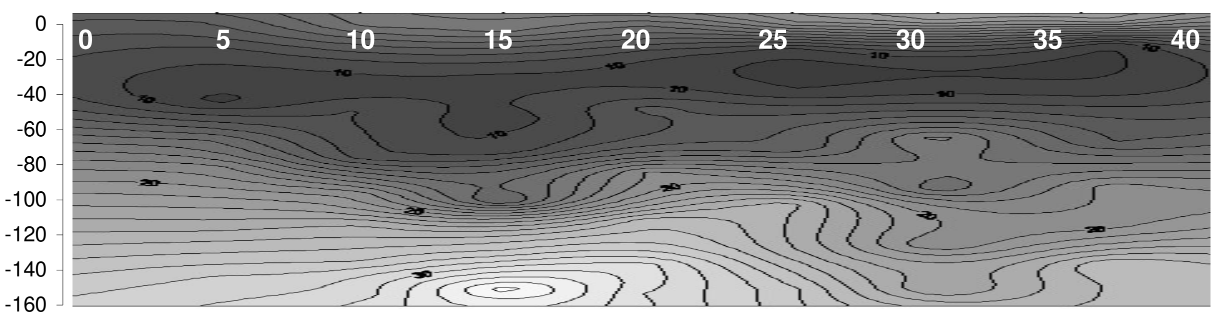

13,0 – 13,40

Gravimetric moisture profiles for selected transects (y axis in cm, x axis in meters)

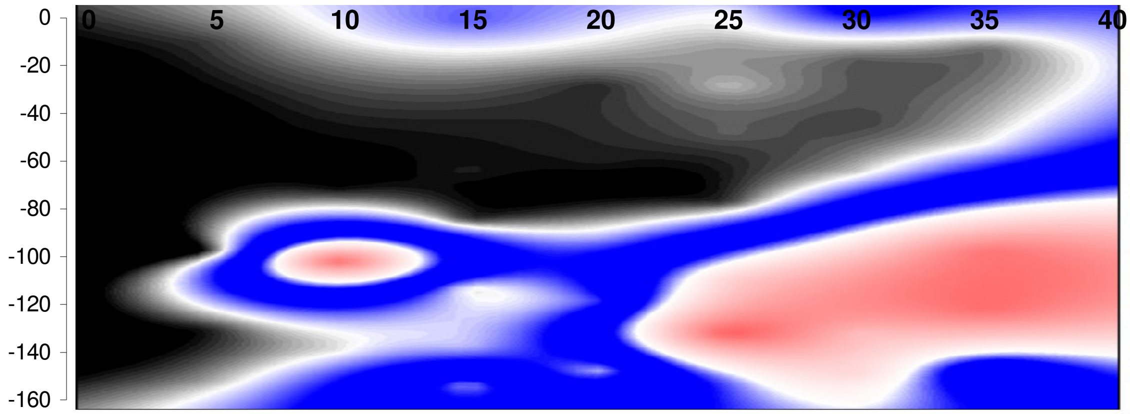

3,0 –3,40

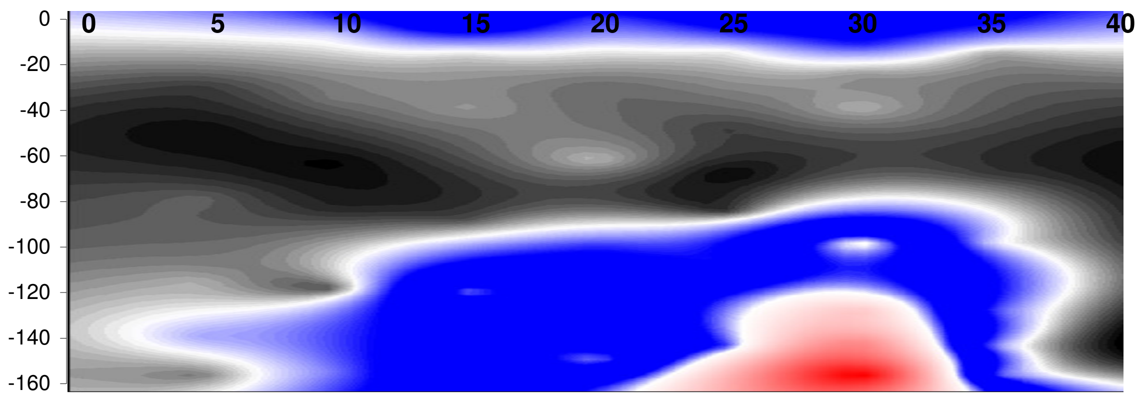

8,0 – 8,40

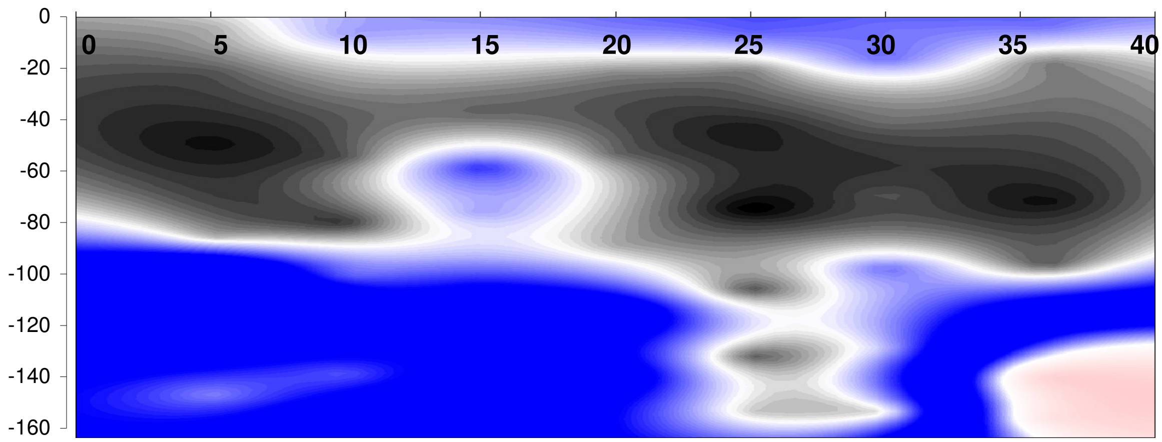

13,0 –13,40

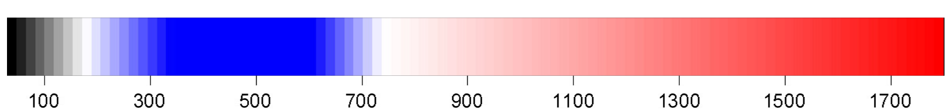

Electrical conductivity profiles for selected transects (y axis in cm, x axis in meters)

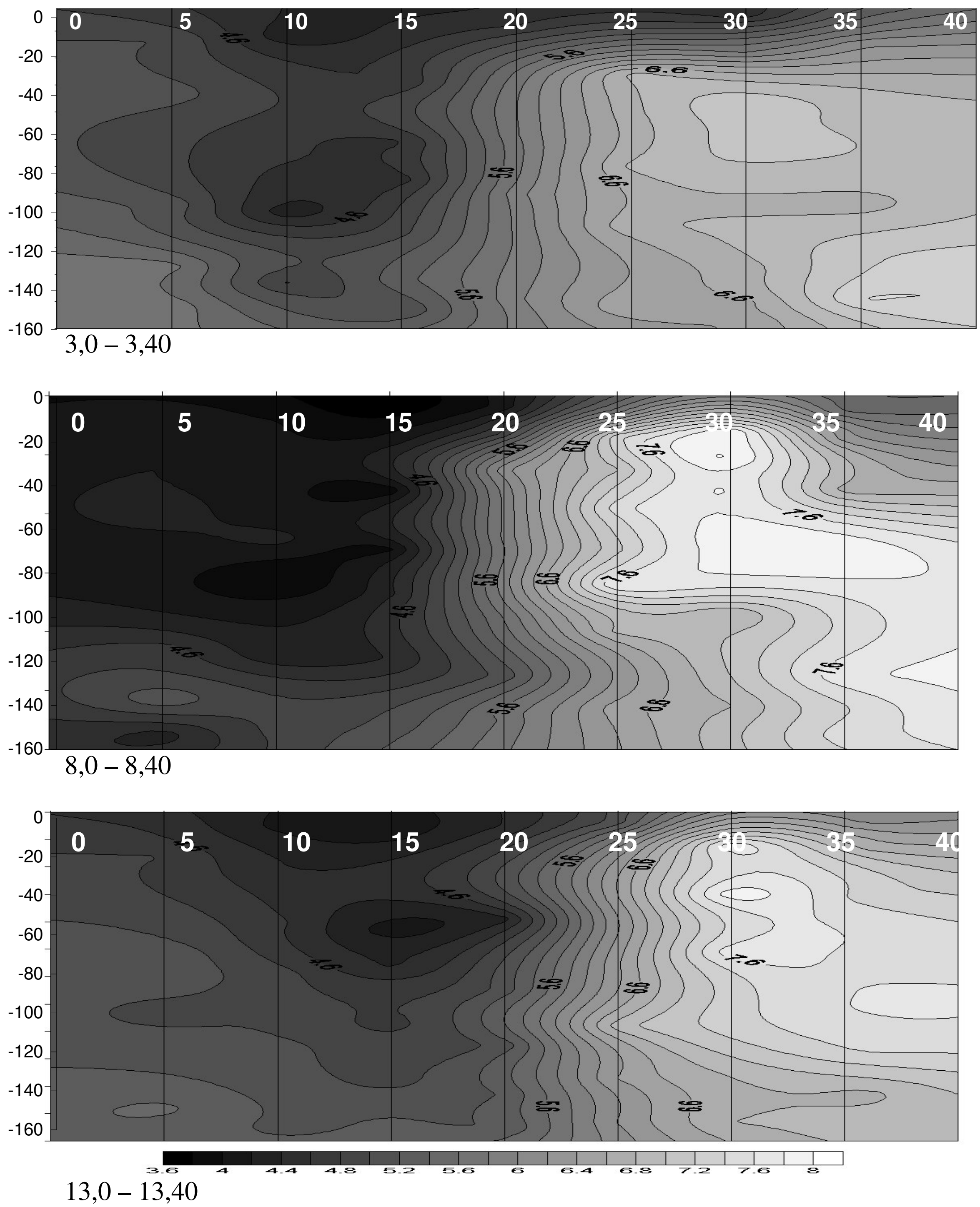

pH profiles for selected transects (y axis in cm, x axis in meters)

APPENDIX F

SOIL PARTICLE DISTRIBUTION

(m)		horizon (cm)					Frac %					
x	y	start	end	Clay	Silt	Sand	v. coarse	coarse	med	fine	v. fine	med:fine
3	15	0	18	13.0	8.6	76.3	0.1	0.6	9.1	87.1	3.1	0.10
3	15	18	56	4.6	5.6	87.6	0.1	0.9	8.5	88.8	1.7	0.10
3	15	56	74	2.4	5.3	89.4	0.0	0.8	7.3	89.8	2.1	0.08
3	15	74	91	4.2	5.7	87.8	1.8	0.9	8.7	86.8	1.8	0.10
3	15	91	124	3.5	2.3	91.6	0.3	0.9	7.6	89.9	1.3	0.08
3	15	124	135	1.1	4.1	92.9	0.0	0.8	9.6	88.3	1.3	0.11
3	15	135	152	1.0	3.0	94.2	0.8	2.4	19.3	76.3	1.2	0.25
3	20	0	20	15.2	9.5	73.6	0.2	0.8	10.3	84.1	4.6	0.12
3	20	20	46	6.2	5.7	85.4	0.1	0.9	8.7	88.3	2.0	0.10
3	20	46	76	5.7	5.6	86.7	0.0	0.8	8.3	89.0	1.9	0.09
3	20	76	102	7.5	3.4	87.1	0.0	0.8	6.6	90.9	1.7	0.07
3	20	102	124	5.7	2.7	90.3	0.1	1.8	13.0	83.5	1.5	0.16
3	20	124	152	1.4	7.7	92.9	0.0	2.4	12.2	84.3	1.0	0.15
3	25	0	10	12.6	8.8	75.5	0.5	0.6	9.6	88.9	0.4	0.11
3	25	25	41	7.0	7.8	82.7	0.3	1.1	10.3	86.7	1.6	0.12
3	25	41	61	6.1	7.4	83.4	0.1	0.7	9.0	88.1	2.0	0.10
3	25	61	91	2.8	6.2	88.5	0.1	1.1	9.5	87.2	2.0	0.11
3	25	91	117	15.6	1.6	81.0	0.5	1.4	9.5	87.2	1.3	0.11
3	25	117	132	15.4	1.0	81.9	0.0	0.8	10.0	88.1	1.1	0.11
3	25	132	152	5.9	1.0	91.8	0.3	4.1	28.1	66.4	1.1	0.42
3	30	0	10	23.3	16.0	56.6	0.1	0.8	9.0	78.3	11.8	0.11
3	30	10	36	5.1	6.3	85.8	0.1	1.2	10.5	86.1	2.2	0.12
3	30	36	58	3.3	3.3	88.4	0.4	1.0	8.8	87.8	1.9	0.10
3	30	58	71	3.3	3.2	86.5	0.1	0.9	9.9	87.0	2.0	0.11
3	30	71	117	15.9	5.6	76.6	0.4	0.8	8.1	88.7	1.9	0.09
3	30	117	132	14.3	1.4	83.1	0.0	1.9	15.9	81.2	1.0	0.20
3	30	132	147	5.9	0.8	92.3	0.0	1.2	22.8	75.3	0.8	0.30
3	30	147	152	4.0	1.1	93.9	0.0	1.3	24.8	73.2	0.7	0.34

(m)		horizon (cm)					Frac %					
x	y	start	end	Clay	Silt	Sand	v. coarse	coarse	med	fine	v. fine	med:fine
8	15	0	10	16.8	9.8	70.6	0.1	1.2	8.5	87.1	3.2	0.10
8	15	10	28	5.0	6.1	85.2	0.0	0.6	8.0	89.5	1.9	0.09
8	15	28	53	5.7	5.9	85.7	0.2	0.9	8.9	88.5	1.5	0.10
8	15	53	79	3.2	5.0	87.5	0.0	0.9	8.2	89.4	1.5	0.09
8	15	79	91	8.2	4.6	84.4	0.1	0.6	8.2	90.1	1.0	0.09
8	15	91	135	6.4	5.1	86.2	0.0	0.9	8.9	87.3	2.8	0.10
8	15	135	152	2.6	2.3	92.5	0.2	0.4	15.4	83.2	0.8	0.19
8	20	0	10	14.1	8.0	75.1	0.0	0.7	9.5	87.2	2.6	0.11
8	20	10	23	8.6	5.9	83.6	0.1	1.3	10.3	86.3	1.9	0.12
8	20	23	41	7.2	5.3	85.5	0.0	0.8	9.3	88.5	1.4	0.11
8	20	41	81	10.6	3.8	83.8	0.3	0.7	8.1	89.4	1.5	0.09
8	20	81	109	9.3	2.8	85.8	0.0	0.4	6.8	91.4	1.4	0.07
8	20	109	127	4.6	1.0	93.1	0.0	1.0	11.2	86.8	1.1	0.13
8	20	127	132	1.8	1.0	95.9	0.0	0.5	13.9	84.9	0.6	0.16
8	20	132	142	3.6	2.0	92.8	0.0	1.3	14.6	83.2	0.9	0.18
8	25	0	13	16.1	10.2	70.6	0.0	0.7	9.6	86.5	3.1	0.11
8	25	13	23	7.0	8.9	82.4	0.9	1.0	9.8	85.8	2.6	0.11
8	25	23	41	6.9	6.6	84.2	0.0	0.6	8.8	88.1	2.4	0.10
8	25	41	56	3.9	6.6	87.2	0.7	0.8	8.7	87.5	2.3	0.10
8	25	56	76	2.2	6.9	88.7	0.0	0.7	9.3	87.7	2.4	0.11
8	25	76	86	4.9	6.7	86.0	0.2	0.8	9.4	87.6	1.9	0.11
8	25	86	117	15.7	1.5	80.9	0.1	2.8	13.6	82.4	1.0	0.17
8	25	117	152	6.7	5.1	88.7	0.0	0.7	18.0	80.7	0.6	0.22
8	30	0	10	16.6	9.6	67.1	0.1	0.8	8.1	81.8	9.2	0.10
8	30	10	20	0.6	21.0	76.9	3.0	1.7	9.0	81.3	5.0	0.11
8	30	20	48	5.0	7.8	84.7	0.6	1.2	8.3	87.2	2.6	0.10
8	30	48	74	2.9	6.3	87.9	0.2	0.7	8.8	87.9	2.4	0.10
8	30	74	114	19.4	3.7	74.4	0.0	0.5	9.2	88.9	1.5	0.10
8	30	114	127	18.4	0.4	79.3	0.1	0.8	10.9	87.0	1.2	0.12
8	30	127	140	13.0	1.2	84.4	0.0	0.8	12.2	85.9	1.1	0.14
8	30	140	152	10.5	2.2	87.4	0.1	1.0	15.2	82.8	0.9	0.18

(m)		horizon (cm)					Frac %					
x	y	start	end	Clay	Silt	Sand	v. coarse	coarse	med	fine	v. fine	med:fine
13	15	0	18	11.4	6.3	79.8	1.4	0.6	9.1	86.7	2.2	0.10
13	15	18	51	5.0	4.8	88.0	0.1	0.8	7.8	89.9	1.5	0.09
13	15	51	58	5.2	3.2	89.1	0.0	0.9	9.8	88.2	1.1	0.11
13	15	58	84	5.1	2.1	89.3	0.0	0.4	6.7	91.6	1.2	0.07
13	15	84	112	4.2	3.2	90.8	0.1	1.0	9.9	87.8	1.1	0.11
13	15	112	137	3.4	2.1	91.7	0.3	0.8	8.6	89.3	1.0	0.10
13	15	137	152	0.6	3.1	94.0	0.0	0.7	14.7	84.1	0.5	0.17
13	20	13	28	7.5	5.5	83.7	0.3	0.7	7.1	89.5	2.4	0.08
13	20	28	71	8.6	4.0	85.5	0.0	0.6	10.6	87.6	1.2	0.12
13	20	71	94	11.3	3.1	83.6	0.0	0.7	8.0	89.9	1.3	0.09
13	20	94	122	8.9	3.4	85.4	0.2	0.9	9.3	88.1	1.5	0.11
13	20	122	140	3.0	3.2	92.3	0.2	2.6	20.8	75.8	0.5	0.27
13	20	140	152	2.4	1.8	94.2	0.0	2.7	18.6	77.9	0.9	0.24
13	25	0	10	17.1	9.1	70.4	0.2	0.6	7.0	79.4	12.7	0.09
13	25	28	53	4.4	6.2	87.2	0.2	0.9	9.6	87.1	2.2	0.11
13	25	53	86	2.3	6.1	89.2	0.0	1.3	9.8	86.7	2.1	0.11
13	25	86	112	7.4	2.7	88.2	0.0	0.8	8.6	89.3	1.4	0.10
13	25	112	135	8.0	1.0	89.8	0.0	2.4	13.7	82.8	1.0	0.17
13	25	135	152	7.8	2.3	87.7	0.3	1.0	15.7	81.9	1.1	0.19
13	30	0	8	16.4	13.5	69.7	0.7	1.9	10.1	79.7	7.6	0.13
13	30	8	23	8.9	9.1	80.1	1.0	1.5	9.8	83.9	3.8	0.12
13	30	23	53	6.0	7.2	86.1	0.0	1.2	9.3	87.1	2.4	0.11
13	30	53	76	4.3	6.9	88.2	0.3	1.0	8.6	87.9	2.2	0.10
13	30	76	107	17.3	0.6	81.0	0.0	0.4	7.0	90.9	1.7	0.08
13	30	107	135	10.4	0.3	89.6	0.0	0.6	11.3	87.0	1.1	0.13
13	30	135	152	6.7	0.9	92.4	0.0	0.5	14.3	84.0	1.2	0.17

APPENDIX G

GROUND-PENETRATING RADAR TRANSECTS

The following profiles are unprocessed ground-penetrating radar transects performed on the grid. The original copies are archived as .dzt files, again, unprocessed. The setup parateters are as follows:

Head Unit: GSSI Sir 2

Antennae: 500MHz

Range: 60 ns

Gains: (linear) -5, 21, 45, 60, 73

Scans/Second: 32

Samples/Scan: 512

Bit/Sample: 8

Filters:

Vertical High Pass: 30MHz

Vertical Low Pass: 1000MHz

Horizontal Smoothing: 4 Scans

Horizontal Background Removal: 0

File names: File1.dzt, File2.dzt, File3.dzt, File4.dzt, File5.dzt, File6.dzt, File7.dzt, File8.dzt, File9.dzt, File10.dzt, File11.dzt, File12.dzt, File13.dzt, File14.dzt, File15.dzt, File16.dzt (file names correspond to transect number +1 (i.e. File1.dzt = transect 0,x)

0,0 – 0,40

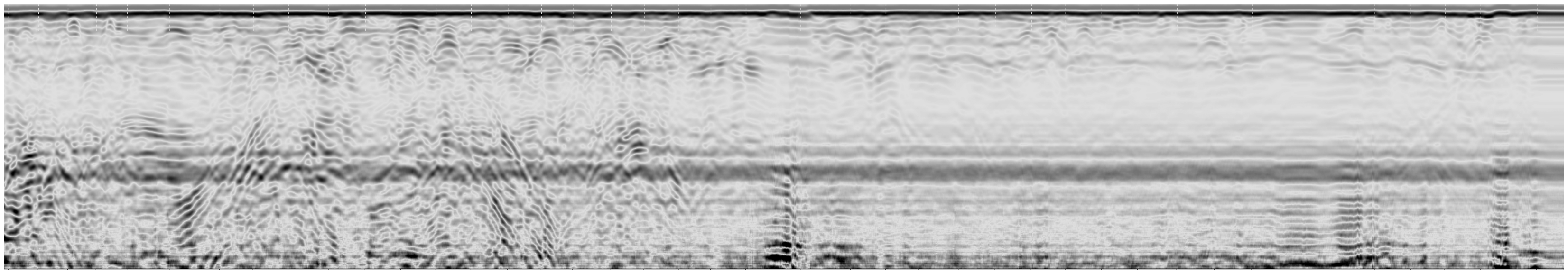

1,0 – 1,40

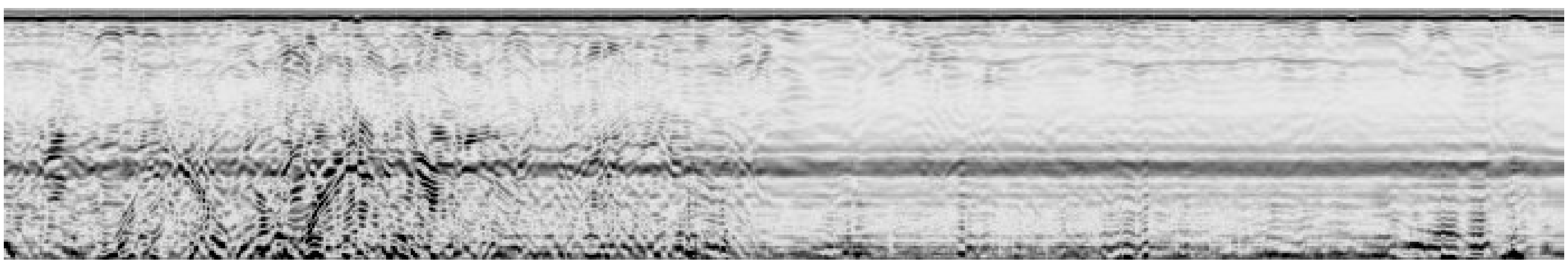

2,0 – 2,40

3,0 – 3,40

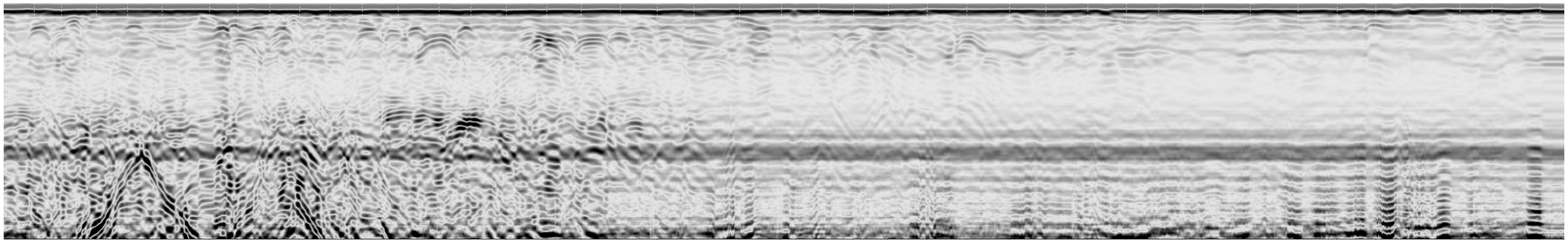

4,0 – 4,40

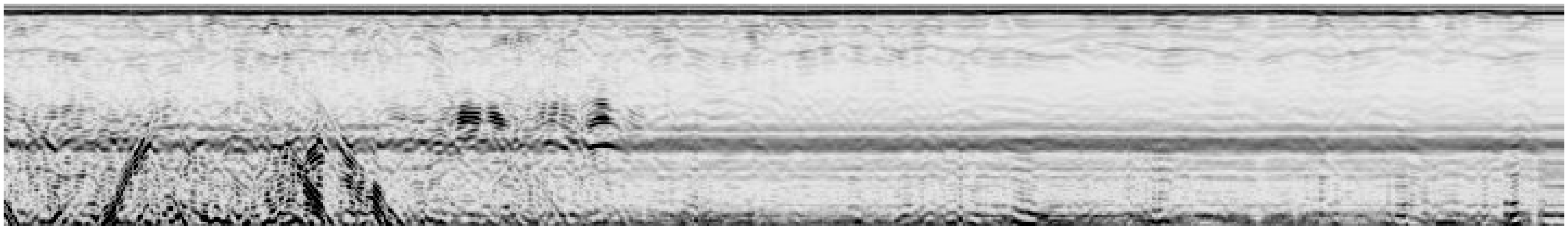

5,0 – 5,40

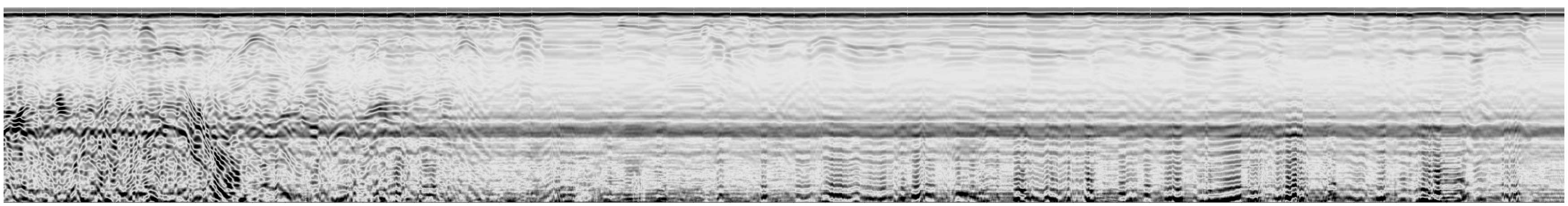

6,0 – 6,40

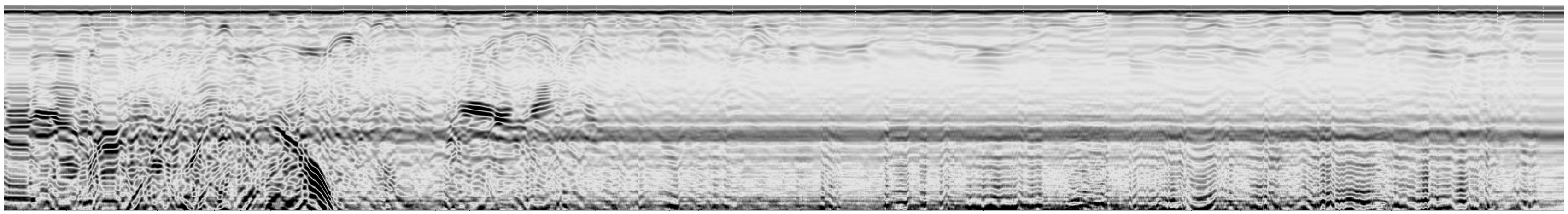

7,0 – 7, 40

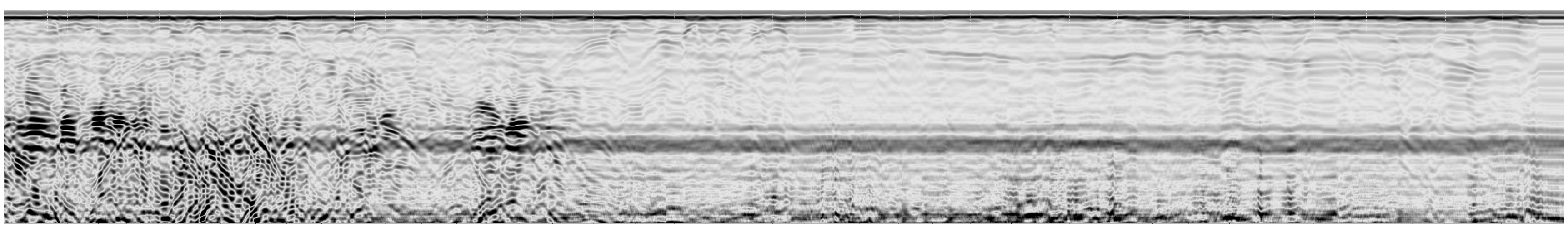

8,0 – 8,40

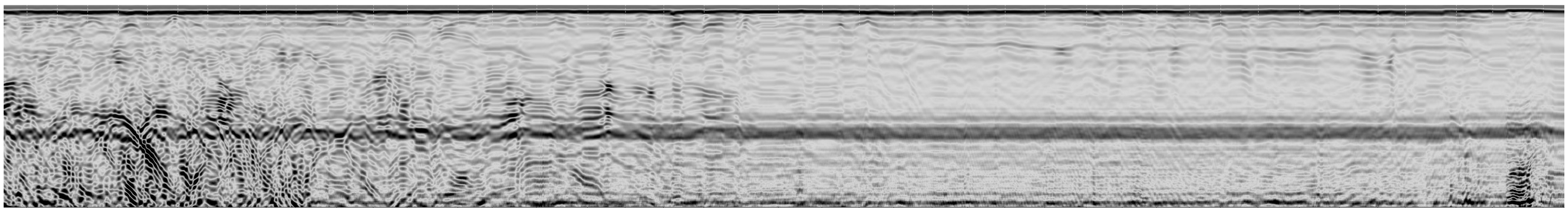

9,0 – 9,40

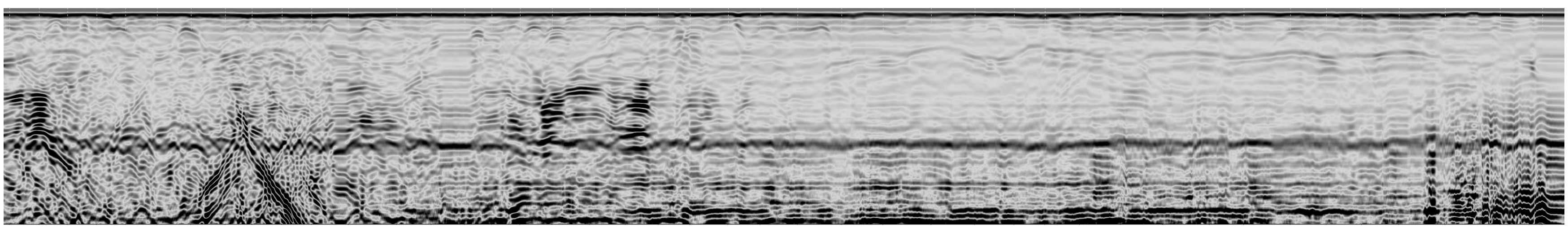

10,0 – 10,40

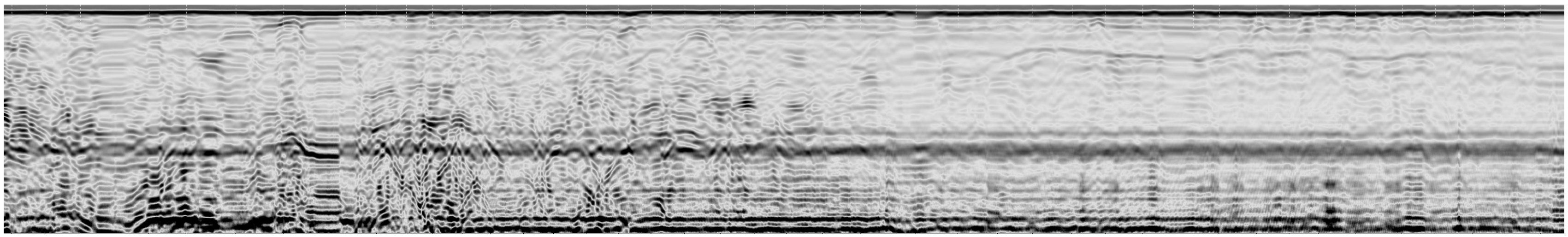

11,0 – 11,40

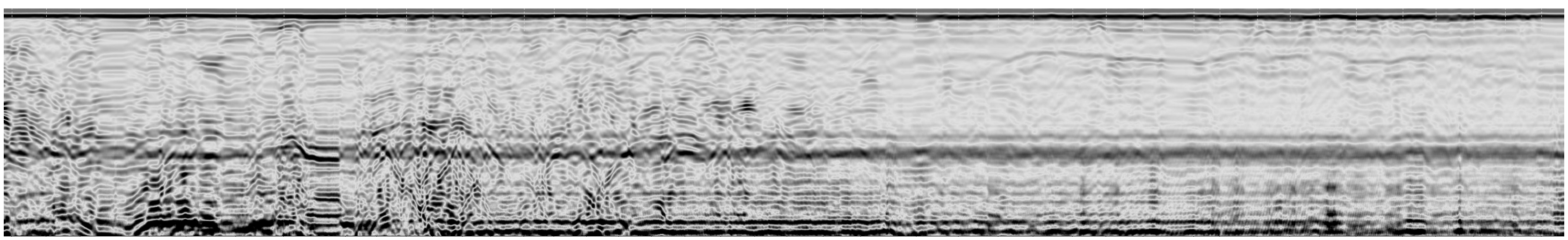

12,0 – 12,40

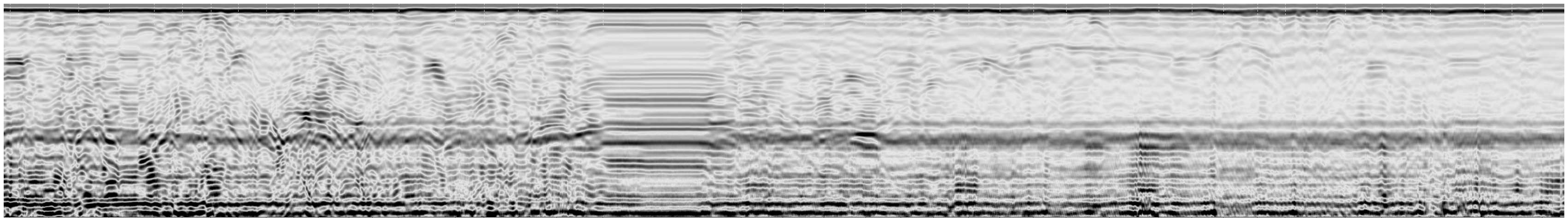

13,0 – 13,40

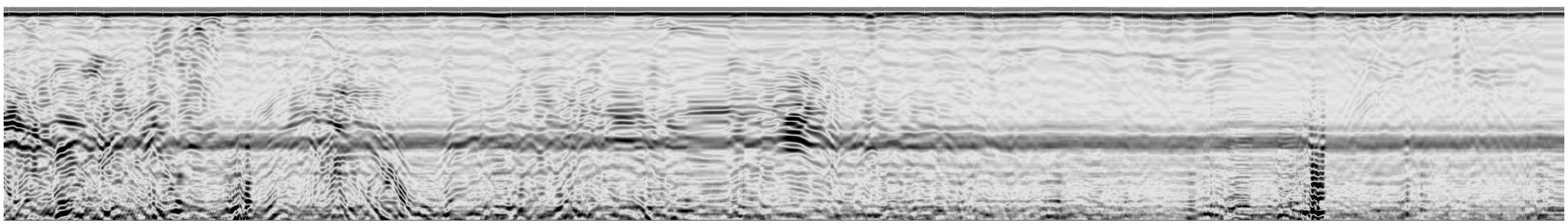

14,0 – 14,40

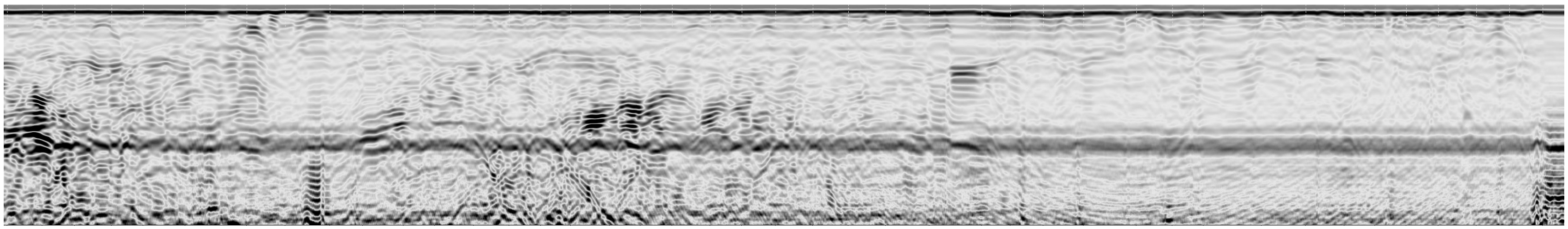

15,0 – 15,40